LAPPEENRANTA-LAHTI UNIVERSITY OF TECHNOLOGY LUT
LUT School of Energy Systems
Degree Programme in Energy Technology

Ida Mäkelä

CALCULATION COMPARISON OF WASTE HEAT RECOVERY BOILER DIMENSIONING TOOLS FOR GAS TURBINE APPLICATION

Examiners: Professor, D.Sc. (Tech.) Esa Vakkilainen
D.Sc. (Tech.) Jussi Saari
Supervisor: M.Sc. (Tech.) Mikko Purhonen

ABSTRACT

Lappeenranta-Lahti University of Technology LUT
LUT School of Energy Systems
Degree Programme in Energy Technology

Ida Mäkelä

Calculation comparison of waste heat recovery boiler dimensioning tools for gas turbine application

Master's thesis

2019

85 pages, 30 figures, 6 tables and 2 appendices

Examiners: Professor, D.Sc. (Tech.) Esa Vakkilainen
Postdoctoral researcher, D.Sc. (Tech.) Jussi Saari
Supervisor: M.Sc. (Tech.) Mikko Purhonen

Keywords: gas turbine, waste heat recovery, dimensioning, heat transfer

Gas turbine combined cycles are used to increase the efficiency and power output of gas turbine power plants. These solutions are often used as peak load power plants, where short start up time and high power-output are the main parameters. Finned tubes are normally used in gas turbine waste heat recovery solutions and so it is also in this Master's Thesis. The used fin model in this study was spiral serrated fin.

Objective of this Master's Thesis was to compare four dimensioning tools that were property of Alfa Laval Aalborg Oy and create a new calculation tool for gas turbine waste heat recovery solutions to be part of the sales tool. Waste heat recovery boilers can be designed with LMTD- or NTU-method. LMTD-method is used when the fluid inlet and outlet temperatures are known, or they can be solved from energy balances. If only inlet temperature is known the effectiveness -NTU -method, should be used.

Two excel-based dimensioning programs, GE2-Select and EGB GS 1999 were examined carefully and the way of calculation were analyzed. The calculation comparison was made within four old calculation tools. Two of them were left out from the comparison, because they were old fashioned and hard to use. The result of the comparison was that none of the programs worked perfectly. Calculation comparison were made for nine cases with EGB GS 1999 and GE2-Select. Results of heat transfer surface and number of tubes differed markable from each other. Calculation of the exhaust gas pressure drop in EGB GS 1999 did not take mass flow rate of exhaust gas into account and therefore it was constant for all nine cases. The result of the comparison was that GE2-Select gives more accurate and sensible results than EGB GS 1999. The aim creating a new dimensioning tool was to solve some problems with the old ones. Therefore, both GE2-Select and EGB GS 1999 were used as a base of calculation in new dimension tool in sales program.

TIIVISTELMÄ

Lappeenrannan-Lahden teknillinen yliopisto LUT
LUT School of Energy System
Energiatekniikan koulutusohjelma

Ida Mäkelä

Kaasuturbiinien jälkeisten lämmöntalteenottokattiloiden mitoitusohjelmien laskennallinen vertailu

Diplomityö

2019

85 sivua, 30 kuvaa, 6 taulukkoa ja 2 liitettä

Tarkastajat: Professori, TkT Esa Vakkilainen
Tutkijatohtori, TkT Jussi Saari
Ohjaaja: DI Mikko Purhonen

Hakusanat: kaasuturbiini, lämmöntalteenotto, mitoitus, lämmönsiirto

Kaasuturbiini kombivoimalaitoksia käytetään tehokkuuden ja tuotetun tehon kasvattamiseksi. Kaasuturbiinivoimalaitoksia käytetään usein huippuvoimalaitoksina, joissa nopea käynnistyminen ja korkea tehontuotanto ovat tärkeitä parametrejä. Ripaputkia käytetään tavallisesti kaasuturbiinien lämmöntalteenottosovelluksissa ja niitä käytetään myös tässä diplomityössä. Tässä työssä käytetty ripa tyyppi on spiraali-lappuripa.

Tämän diplomityön tavoitteena oli vertailla neljää Alfa Laval Aalborg Oy:n mitoitusohjelmaa ja luoda uusi laskentaohjelma kaasuturbiinien lämmöntalteenotto sovelluksille. Lämmöntalteenottokattat voidaan mitoittaa käyttäen apuna joko LMTD- tai NTU-metodia. LMTD-metodia käytetään kun fluidin molemmat sekä sisääntulo että ulosmeno lämpötilat ovat tiedossa tai ne voidaan selvittää energiatasapainoyhtälöistä. Jos vain fluidin sisäänmenolämpötila on tiedossa tulisi käyttää NTU-metodia.

Kahta excel-pohjaista mitoitusohjelmaa, GE2-Select:iä ja EGB GS 1999:a, tarkasteltiin tarkemmin ja niissä käytettyä laskentatapaa analysoitiin. Laskennallinen vertailu suoritettiin neljän vanhan laskentaohjeman välillä. Kaksi ohjelmaa jätettiin pois vertailusta, koska ne olivat vanhanaikaisia ja vaikeakäyttöisiä. Laskennallinen vertailu tehtiin yhdeksälle tapaukselle EGB GS 1999 ja GE2- Select ohjelmia käyttäen. Lämmönsiirtoalan ja putkien lukumäärän tulokset vaihtelivat merkittävästi toisistaan. EGB GS 1999 savukaasun painehäviön laskenta ei ottanut huomioon savukaasun massavirtaa ja se oli vakio kaikille yhdeksälle tapaukselle. Vertailun tulos oli, että GE2-Select antaa todenmukaisemmat ja järkevämmät tulokset. Tulokseksi saatiin, että mikään ohjelmista ei toimi täydellisesti. Uuden laskentatyökalun kehittämisen tarkoituksena oli ratkaista joitakin ongelmia, joita vanhoissa oli. Tämän vuoksi molempia GE2-Selecti:ä ja EGB GS 1999 käytettiin pohjana myyntiohjelman uuden työkalun luonnissa.

ACKNOWLEDGEMENTS

This Master's thesis was written for Alfa Laval Aalborg Oy during the Spring 2019. Writing this thesis has been a great learning process for me and I would like to thank Alfa Laval Aalborg Oy and especially Pekka Läiskä for this subject for my thesis. I would also like to thank my supervisor Mikko Purhonen for advices and support during this process. Furthermore, I would like to thank Jori Rantanen for opportunity to work in Service project team at the same time I have done my thesis.

I would like to thank examiners of this thesis Esa Vakkilainen and Jussi Saari for examining my work and for great and interesting courses during this 5-year journey. Armatuuri ry was my second home during my studies and from this group of people I have gotten the best friends of mine. Thank you, our dear guild, for that. Finally, I would like to express my gratitude to my friends and family who have supported me whatever I decide to do.

In Rauma on 17th of May 2019

Ida Mäkelä

CONTENTS

LIST OF SYMBOLS AND ABBREVIATIONS

Roman alphabet

A	area	m^2
c_p	constant specific heat	kJ/kgK
C	heat capacity rate	J/K
C_1	constant 1	-
C_2	constant 2	-
C_3	constant 3	-
C_r	heat capacity ratio	-
dA_s	element surface area difference	m^2
dq	heat transfer rate difference	-
dT	temperature difference	K
dx	difference of the distance	m
h	heat transfer coefficient	$W/(m^2K)$
H	enthalpy	kJ/kg
k	thermal conductivity	W/mK
L	distance	m
m	constant 4	-
n	constant 5	-
N	number of	-
P	power required	kW
q	heat transfer rate	W/mK
q_m	mass flow rate	kg/s
q''_x	heat flux	W/m^2
Q	heat power	kW
r	radius	m
R_t	thermal resistance	$W/(m^2K)$
T	temperature	K
$T(x)$	temperature at x	K
U	overall heat transfer coefficient	W/m^2K

v	specific volume	m^3/kg
V	velocity of the fluid	m/s
x	distance	m

Greek alphabet

η	efficiency	-
ε	effectiveness	-
ρ	density	kg/m^3
μ	viscosity	Pa·s

Dimensionless numbers

Nu_D	Nusselt number	-
Re_D	Reynolds number	-
Pr	Prandtl number	-

Subscripts

1	before compressor
2	after compressor
3	after combustion chamber
4	after turbine
7	before steam turbine
8	after steam turbine
a	air
A	material A
b	bottoming cycle
B	material B
c	cold
cc	combined cycle
comb	combustion chamber
comp	compressor
cond	conduction
conv	convection

cross	cross-sectional area
f	flue
fin	fin
g	gas
h	hot
HE	heat exchanger
in	inlet
max	maximum
min	minimum
net	net
o	overall
out	oulet
s	steam
st	steam turbine
shell	shell passes
t	turbine
T	tube
Ts	at surface temperature
th	thermal
tot	total
x+dx	at x+dx
∞	fluid

Abbreviations

CO_2	Carbon dioxide	
EG	Exhaust Gas	
ERP	Enterprise Resource Planning	
HRSG	Heat Recovery Steam Generator	
IMO	International Maritime Organization	
LCV	Lower Caloricfic Value of the fuel	kJ/kg
LMTD	Log Mean Temperature Difference	

MGTC	Maisotsenko Gas Turbine Cycle
NO_x	Nitrogen oxides
NTU	Number of heat Transfer Units
ORC	Organic Rankine Cycle
SO_x	Sulfur oxide
WHR	Waste Heat Recovery

1 INTRODUCTION

Storing electricity on a large scale is not possible nowadays. Therefore, electricity should be produced when it is needed, maintaining the balance between demand and supply. This can be done by using gas turbine waste heat recovery systems. Both investment costs and environmental impacts are often relatively low, while the overall efficiency remains high and construction times short. Designing gas turbine combined cycle is optimization between costs and benefits. The biggest cost in Heat Recovery Steam Generator (HRSG) boiler is installation of the heat exchange surface. The main indicator dimensioning the size of the heat transfer surface is the pinch point in the evaporator. (Kehlhofer et al. 2009, 5-6; 190.)

Gas turbines can be part of a combined cycle which can be defined as a combination of two thermal cycles. Efficiency of a combined cycle is higher than a simple gas turbine process. Cycle with higher temperature is called topping cycle, where heat is produced; in gas turbine – scenarios, the gas turbine process is the topping cycle. Waste heat is used in the bottoming cycle which is on a lower temperature level. (Kehlhofer et al. 2009, 1-2.)

In Alfa Laval Aalborg waste heat recovery boilers that are examined in this thesis, water flows in the tubes and exhaust gas flows on the shell side of the boiler. Tubes are finned with solid or serrated fins. Calculation programs that are compared in this thesis, are for spiral finned tubes. Fins add heat transfer area and make heat transfer more efficient. Heat transfer in a waste heat recovery -boiler depends more on properties of exhaust gases and external heat transfer than internal heat transfer inside the tubes on the water side.

1.1 Objectives and background of the thesis

The objective of this thesis is to examine Waste Heat Recovery (WHR) solutions for gas turbines applications at Alfa Laval Aalborg Oy. Two different dimensioning programs that have been used for WHR-boiler sales in the past are analyzed and compared to each other and to the literature. Correlations and other equations are analyzed. Possible shortcomings in the programs are determined and corrective proposals are presented.

Effect of radiation in these practical solutions is evaluated and need of it in dimensioning is analyzed. Different possible solutions for waste heat recovery after gas turbines are presented and theoretical calculations are defined.

One main target of the thesis is to create an update block to the sales tool and make it as efficient as possible. Sales tool includes many different sales and dimensioning programs in addition to boiler dimensioning and budget calculations. Other main functions of the sales tool are the creation of technical specifications and transferring information to Enterprise Resourcing Planning tools (ERP). Different technical solutions can be designed with the sales tool at the moment. Goal for this thesis is to implement a specific dimensioning tool for spiral tube serrated fin application to the sales tool.

Target in this dimensioning tool is to design the most economical and efficient solution for each gas turbine combined cycle project. Dimensioning is done with both Log Mean temperature and Number of heat Transfer Units -methods (LMTD- and NTU-methods), and different tube banks of the boiler, such as superheaters, evaporators and economizers, are dimensioned separately. Dimensioning tool is a harmonious part of the sales program and uses some already existing parts of it while calculating.

1.2 Structure of the thesis

Chapter 2 includes general explanation of gas turbine combined cycles, low temperature economizers and Organic Rankine Cycles (ORC). A special application of Maisotsenko gas turbine bottoming cycle is also presented. Basic calculation of the thermodynamic system of gas turbine combined cycle is presented and defined.

Chapter 3 presents theoretical calculation procedures of heat transfer starting with a plane wall and moving on to a cylinder and finned tubes. Overall surface efficiency is presented, and external flow in tubes and tube banks are defined. Both NTU- and LMTD-methods are presented. Internal flow in tubes is explained and related equations are presented.

Chapter 4 considers two different dimensioning programs that have been used by Alfa Laval Aalborg Oy. First dimensioning program is GE-2 Select and second EGB GS 1999. Also, effects of radiation for heat transfer of finned tubes is explained. Dimensioning programs

are compared to each other and their efficiency is evaluated. Calculation comparison is made with nine cases for dimensioning tools. Results of the comparison are presented in the diagrams. Equations are presented in Appendices 1-2. Appendices 1 and 2 are property of Alfa Laval Aalborg and are not included in the public version of the thesis.

Chapter 5 includes a general explanation of Alfa Laval Aalborg's dimensioning and sales program. The procedure of updating gas turbine waste heat recovery boiler dimensioning section to sales tool is defined and explained. Chapter 6 presents conclusions based on the analyses in this thesis, with some possible further research on this topic is also presented in this chapter.

2 WASTE HEAT RECOVERY BOILERS FOR GAS TURBINES

Gas turbine process, also referred to as Brayton process, consists of three main phases. First combustion air is compressed. Second, the compressed air is led into the combustion chamber where fuel is added to the process through nozzles. Finally, flue gas is expanded in the turbine. Two thirds of the produced energy is consumed as work of the compressor. Efficiency of the process is dependent of temperature in the combustion chamber and pressure ratio of the turbine. (Raiko et al 2002, 557.) (Kehlhofer et al. 2009, 165.)

Gas turbines are commonly used in aircraft propulsion and power generation. Often gas turbines are used in combined cycle systems. These bottoming cycles can be with steam or air. Bottoming cycles are used to utilize waste heat from the exhaust gases of the gas turbine. Power output and efficiency of the simple gas turbine process can be increased with these waste heat recovery solutions. (Khan et al. 2017, 4547.) In figure 2.1 the simple gas turbine process is showed.

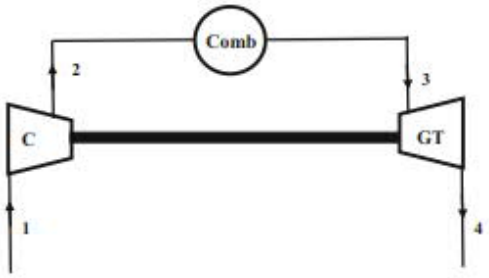

Figure 2.1: Simple gas turbine process (Khan et al. 2017, 4549.)

Also, regulations for emissions to the atmosphere have become a more and more crucial issue in recent years in ship production by International Maritime Organization (IMO) standards. Restrictions are made because of controlling planet's greenhouse effect. Legislation is focused mainly on sulfur oxides (SO_x), nitrogen oxides (NO_x) and carbon dioxide (CO_2). The amount of emitted carbon dioxide can be reduced by using fuels with low carbon content or using a more efficient engine system. There is always some uncertainty with costs of fuels and from an economic perspective it is most reliable to search for the most efficient engine system. Waste heat recovery can be organized with HRSG heat exchangers, pumps, steam turbine and electric machinery. (Altosole et al. 2017, 1-2.)

Efficiency of thermal power plants can be increased by recovering heat from exhaust gases at the cold end of the process. Heat recovery is used to decrease the amount of utilized fuels and achieve a higher efficiency in power generation. (Youfu et al 2016, 1118.) Heat recovery from the gas turbine can be utilized by a combined cycle plant, where the gas turbine generates approximately 2/3 of the total power output. (Kehlhofer et al. 2009, 165.)

One choice for waste heat recovery system for gas turbine is organic Rankine cycle, where the working fluid is an organic compound instead of water/steam. ORC is a good option for low and medium temperature exhaust gases. In this system it is not possible to produce steam, but the generation of electricity is possible. Organic Rankine cycle can be more efficient than traditional water/steam cycle system, because the thermal efficiency of water is low, and the volume of the flow must be large. (Carcasci et al. 2014, 91.)

2.1 Gas turbine combined cycles

There is a variety of different arrangements. One arrangement is a new thermodynamic energy cycle. This cycle is used with multicomponent working agents. New thermodynamic cycle can be used as bottoming cycle in combined cycle system. It can also be used to generate electricity from low temperature heat sources. Another arrangement is a novel gas turbine power plant where carbon oxide is captured during combustion, which increases the thermal efficiency of the system. (Khan et al. 2017, 4547.)

Gas turbine produces exhaust gases that can be utilized in a bottoming cycle. This cycle can operate with a low temperature compared to the topping cycle. The linking part between the gas turbine system and bottoming cycle is a heat recovery steam generator. HRSG system with three-pressure reheat is also researched. The study showed that heat recovery steam generation system’s inlet temperature does not affect the efficiency of the steam system when the temperature is over 590 °C. (Khan et al. 2017, 4548.) Combined system with a HRSG can be seen in figure 2.2.

Gas turbine is the most important component of the combined cycle plant. Development of the component can be done by increasing the turbine inlet temperature and/or compressor air flow. The enthalpy drop increases when the turbine inlet temperature is increased. When

the enthalpy drop is higher, the efficiency of the process and the total power output increases. Generally, the competitiveness of the product and the full potential should be maximized. Increasing the turbine inlet temperature means that the combustion system should generate an exhaust gas temperature as high as possible. Contradictorily, the flame temperature should be low because of the low emission limits. When the flame temperature increases, the emissions of NO_x also increase.

There are two main categories of gas turbines that are used to generate power. First category is aeroderivative gas turbines that are mainly two- or three-shaft turbines with drive turbine and variable-speed compressor. In these so-called jet engines, the turbine inlet temperatures are usually higher than in heavy-duty industrial turbines. The weight of the gas turbine is the most important factor in jet engines. Efficiency of the jet engines are higher than the industrial gas turbine efficiency. Single shaft applications are called heavy-duty industrial gas turbines. In these heavy-duty gas turbines, the major developments have been achieved in the last decade. Nowadays, the biggest invention is a gas turbine with sequential combustion.

Gas turbine with sequential combustion is one application of heavy-duty industrial gas turbines. First in this kind of gas turbine, the compressed air flows to the first combustion chamber. After that, the fuel is combusted to the inlet temperature of the first turbine. Exhaust gases expand in first turbine, generating power before they enter to second combustion chamber. In the second combustion chamber additional fuel is combusted to achieve the gas temperature to inlet temperature of the second turbine. In the second turbine the exhaust gases expand to atmospheric pressure.

Heat Recovery Steam Generator converts the thermal energy in the gas turbine exhaust gases to energy in the steam. First feed water is heated in the economizer and after that the steam enters the drum in a subcooled condition. After that, the feed water enters the evaporator and after that flows back to the drum as a mixture of the water and steam. In the drum the steam and water are separated. Saturated steam flows to the superheater where the steam is heated to the maximum heat transfer temperature. Often there are two or three pressure levels in the system. (Kehlhofer et al. 2009, 183.)

HRSG without supplementary firing is basically a convective heat exchanger. HRSG can be divided to two categories based on the direction of the exhaust gas flow. The first category is vertical HRSG, where exhaust gases flow in a vertical direction outside horizontal heat transfer pipes. In the past vertical HRSG was also called a forced circulation HRSG, because a pump was needed to provide the circulation in different stages in the evaporator. Nowadays, vertical HRSG can also be designed without pumps as natural circulation systems. The other category is horizontal HRSG, where the exhaust gas flows in a horizontal direction. Typically, these HRSGs are known as natural circulation HRSGs because the circulation through evaporators occurs by gravity and density differences. In this type the heat transfer pipes are positioned vertically and are usually self-supporting. Low temperature corrosion is one major thing that has to be under consideration while designing a HRSG boiler. All the surfaces that are in contact with exhaust gases should be in a temperature above the sulfuric acid dew point.

Third main component in a gas turbine combined cycle is the steam turbine. The most important characteristics of the modern combined cycle steam turbine are high efficiency, short installation time, short startup time and a floor mounted configuration. Compared to conventional steam turbines the combined cycle steam turbines have higher power outputs, higher live-steam temperatures and pressures, and more extractions for feedwater heating. Startup times have to be short because plants are usually used as part-load units and they have daily or weekly startups. Often more than one pressure level is used and therefore there are multiple inlets in the steam turbine. Because of this steam mass flow in steam turbine increases between the first inlet and the outlet. (Kehlhofer et al. 2009, 165-196.)

To optimize regular gas turbine process and output of the topping cycle, waste heat energy can be used to heat and boil water in a heat recovery steam generator in the bottoming cycle. In the bottoming cycle, the steam flow rate is chosen based on a given limited power output. In the bottoming cycle, the steam/water mixture after steam turbine is condensed and it circulates back to HRSG via a feed water circulation pump. (Khan et al. 2017, 4550-4551.) This can be seen in figure 2.2.

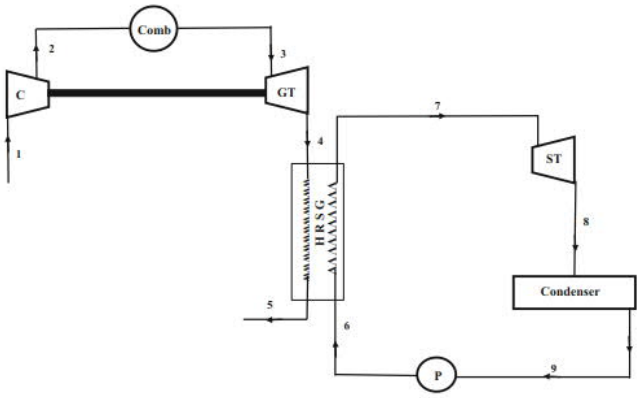

Figure 2.2: Combined gas and steam power cycle with HRSG system (Khan et al. 2017, 4549.)

Also, a combustion air preheater, also called a recuperator, can be added to the cycle. This can be seen in figure 2.3. A heat exchanger is placed between the compressor and the combustion chamber, where it uses exhaust gases from the turbine to preheat combustion air to increase efficiency. (Khan et al. 2017, 4551.)

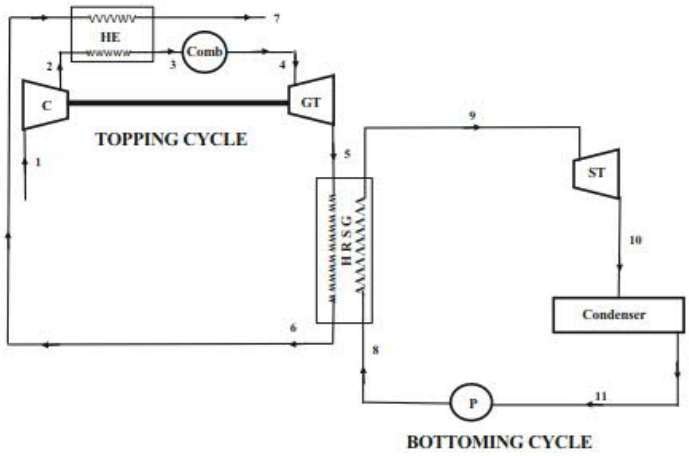

Figure 2.3: Combined gas and steam power cycle with HRSG and recuperator (Khan et al. 2017, 4550.)

All components in the combined cycle can be analyzed. It can be approximated that the pressure losses in equipment are negligible. Also, it can be assumed that the specific heat for the working fluid remains constant despite changes in temperatures. First the air compressor

power is solved. The analysis is in this case made for the process in figure 2.2. (Khan et al. 2017, 4551.)

$$P_c = q_{m,a}(H_1 - H_2) \quad (2.1.1)$$

where P_c power required for the compressor [kW]

$q_{m,a}$ mass flow rate of the air [kg/s]

H_1 air enthalpy before compressor [kJ/kg]

H_2 enthalpy after compressor [kJ/kg]

After the power of the compressor is calculated with equation (2.1.1), the thermal power in the combustion chamber can be defined.

$$Q_{comb} = q_{m,g}H_3 - q_{m,a}H_2 \quad (2.1.2)$$

where Q_{comb} thermal power in combustion chamber [kW]

$q_{m,g}$ mass flow rate of the gas [kg/s]

H_3 enthalpy after combustion chamber [kJ/kg]

Mass flow rate of the fuel to combustion chamber is calculated.

$$q_{m,f} = \frac{H_3 - H_2}{LCV - H_2} \quad (2.1.3)$$

where LCV lower caloric value of the fuel [kJ/kg]

When the power in the combustion chamber is solved with equation (2.1.2), the mass flow rate of the gas can be calculated when the mass flow rates of the fuel and air are known. Mass flow rate of flue can be calculated with equation (2.1.3).

$$q_{m,g} = q_{m,a} + q_{m,f} \quad (2.1.4)$$

where $q_{m,f}$ mass flow rate of the fuel [kg/s]

Power generated in the turbine can be solved after the mass flow rate of the gas is defined with equation (2.1.4).

$$P_{\mathrm{t}} = q_{\mathrm{m,g}}(H_3 - H_4) \tag{2.1.5}$$

where P_{t} power generated in the turbine [kW]

H_4 enthalpy after turbine [kJ/kg]

Net power of the topping cycle can be calculated as the difference between powers of the compressor and turbine, after solving them with equations (2.1.1) and (2.1.5).

$$P_{\mathrm{net}} = P_{\mathrm{t}} - P_{\mathrm{c}} \tag{2.1.6}$$

where P_{net} Net power of the topping cycle [kW]

Thermal efficiency in the topping cycle can be calculated with net power of the cycle and thermal power of the combustion chamber. Net power of the cycle can be calculated with equation (2.1.6).

$$\eta_{\mathrm{th}} = \frac{P_{\mathrm{net}}}{Q_{\mathrm{comb}}} \tag{2.1.7}$$

where η_{th} thermal efficiency of the topping cycle [-]

Thermal efficiency of the topping cycle is solved with equation (2.1.7). Net power of the bottoming cycle can be calculated by calculating the power generated in steam turbine.

$$P_{\mathrm{net,b}} = P_{\mathrm{st}} = q_{\mathrm{m,s}}(H_7 - H_8) \tag{2.1.8}$$

where $P_{\mathrm{net,b}}$ net power in bottoming cycle [kW]

P_{st} power of the steam turbine [kW]

$q_{\mathrm{m,s}}$ mass flow rate of steam [kg/s]

H_7 enthalpy before steam turbine [kJ/kg]

H_8 enthalpy after steam turbine [kJ/kg]

Combined cycle net power can be calculated when the Net power of the bottoming cycle is calculated with equation (2.1.8).

$$P_{\text{net,cc}} = P_{\text{net}} + P_{\text{net,b}} \quad (2.1.9)$$

where $P_{\text{net,cc}}$ net power of the combined cycle [kW]

Thermal efficiency of the whole combined cycle can be calculated when the power of the combined cycle is known. It can be calculated with equation (2.1.9).

$$\eta_{\text{th,cc}} = \frac{P_{\text{net,cc}}}{Q_{\text{comb}}} \quad (2.1.10)$$

where $\eta_{\text{th,cc}}$ thermal efficiency of combined cycle [-]

Thermal efficiency of the combined cycle can be calculated with equation (2.1.10). Effectiveness of the heat exchanger in the topping cycle is solved.

$$\varepsilon_{\text{HE}} = \frac{H_1 - H_2}{H_3 - H_2} \quad (2.1.11)$$

where ε_{HE} effectiveness of the heat exchangers [-]

Effectiveness of the heat recovery steam generator HRSG can be solved after the effectiveness of the heat exchanger is defined with equation (2.1.11).

$$\varepsilon_{\text{HRSG}} = \frac{q_{\text{m,g}}(H_3 - H_4)}{q_{\text{m,g}}H_7 - q_{\text{m,s}}H_8} \quad (2.1.12)$$

where $\varepsilon_{\text{HRSG}}$ effectiveness of the HRSG [-]

The effectiveness of the heat recovery steam generator is calculated with equation (2.1.12). Gas turbine combined cycle is used widely because by using it the reliability of gas turbines can be maximized. Because the system is more reliable, the duration of the scheduled maintenance is minimized. Also, the whole system can be upgraded. (Usune et al. 2011, 54.) Gas turbine combined cycle can be improved in many ways. One way is to improve the

performance of the process in partial load conditions. One solution for this improvement can be a backpressure adjustable gas turbine combined cycle. (Li et al. 2018, 739.)

Heat recovery steam generators can also be used in marine solutions as one- or two-boiler systems. One boiler system can be single-pressure system or dual-pressure system, whereas a two-boiler system must have two pressure levels. Optimization of the marine solution is based on different parameters than in land power plant. The main aspect is to minimize the physical dimensions and increase ship load capacity. (Altosole 2017, 8.) Efficiency of the system must be considered, but the minimizing the size of the components has to be also in balance. (Altosole 2017, 9.) Reduction of carbon dioxide emissions has to be considered. (Altosole 2017, 10).

2.1.1 Maisotsenko gas turbine bottoming cycle

In small scale gas turbine power plants, the conventional combined cycle with both topping and bottoming cycles, is utilized. In this conventional combined cycle system both, a condenser and a HRSG, are located in the bottoming cycle. Therefore, when the capacity of the power plant is 50 MW or less, this conventional system is not the most economical choice. Air turbine cycle integration, called an air bottoming cycle (ABC), also exists. This arrangement has low costs building phase and a relatively short startup time. Operation temperature of this system is high and therefore this system does not fit to be in bottoming cycle. It can be used in the topping cycle where the temperatures are higher, but it does not recover all the waste heat. (Saghafifar & Gadalla 2015, 351.)

Maisotsenko gas turbine cycle (MGTC) is air turbine cycle for humid air. The air for bottoming cycle is humified with an air saturator. Recovery of waste heat occurs by heating air and humidifying the process. The advantages of using humidified air in the process are higher heat capacity and mass of the air. (Saghafifar & Gadalla 2015, 351-352.) Maisotsenko bottoming cycle layout can be seen in figure 2.4.

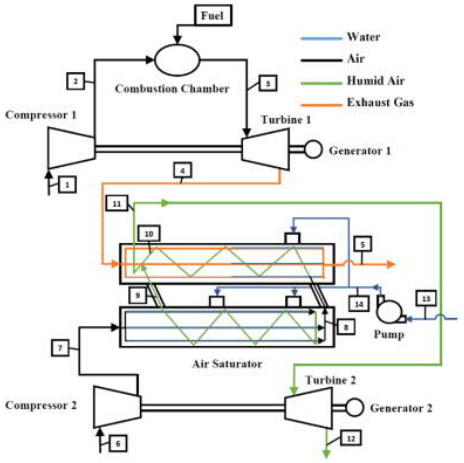

Figure 2.4: Maisotsenko bottoming cycle layout (Saghafifar & Gadalla 2015, 353.)

Gas turbine process with Maisotsenko bottoming cycle in T-s diagram can be seen in figure 2.5. In the state 1 the combustion air is flowing in the compressor in the topping cycle. Between states 1 and 2 the compression is adiabatic. Compressed air flows to combustion chamber where the fuel and air are mixed together. The process between states 2 and 3 is isobaric. After combustion the exhaust gases are flowing to the turbine where they are expanding adiabatically. This work generated in process 3-4 can now be used for power generation in the generator.

Exhaust gases produced in topping cycle are drawn into a system air saturator. The system air is refrigerated to the inlet temperature of the bottoming cycle. (Saghafifar & Gadalla 2015, 352.)

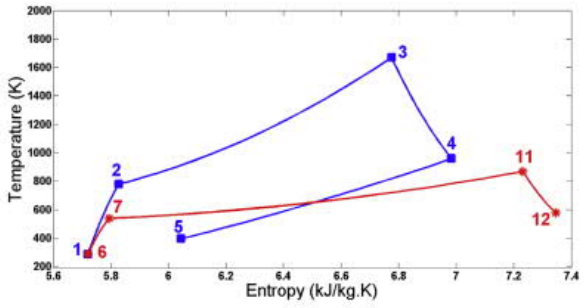

Figure 2.5: Gas turbine process with Maisotsenko bottoming cycle in T-s diagram (Saghafifar & Gadalla 2015, 353.)

In state 6 the combustion air is also led into the compressor and it is compressed in an adiabatic process 6-7. Compressed air is then led into the air saturator and where the system air is heated up and humidified. Between stages 7-11 exhaust gases from the topping cycle are used to humidify the air flow. Air saturator bottom section is used to divide system air to three streams after compression. Between stages 7 and 8 the compressed air is refrigerated.

Two of these three streams are mixed up and led to the upper part of the saturator and the third one fed back to the bottom section. Humidity of the third stream increases in the lower section. Mixed steam heats up on the top section by exhaust gases in process 8-10. At stage 9 humified air steam is mixed and at stage 10 two humified air steams are mixed together. At stage 11 the system air is leaving the saturator. Humid air is expanded in process 11-12 adiabatically. (Saghafifar & Gadalla 2015, 352-353.)

2.2 Low temperature economizer

A low temperature economizer is used to cool exhaust gases and transfer heat to feed water. Finned tubes are used because of their good properties with resisting abrasion. The risk with low temperature economizers is the rapid low temperature acid corrosion and therefore exhaust gas temperature must be between 70 °C and 100°C, where the corrosion rate is as low as possible. Outlet temperature of the low temperature economizer is often designed to be approximately 90 °C. (Youfu et al. 2017, 1119-1120.)

From steam turbine exit steam is condensed and used as feed water after various stages of preheating. Preheating without low temperature economizers is done using high temperature steam. When the waste heat recovery system is installed the feed water is heated with exhaust gases. All the steam that has been used to heat feed water is saved. If the power output before and after waste heat recovery solutions is the same, the amount of the fuel used decreases, simultaneously reducing CO_2 emissions. If the amount of the fuel however stays at the same level, the power output increases. (Wang et al. 2012,197.)

2.3 Organic Rankine cycle

The main components of Organic Rankine Cycle process are an evaporator, a turbine, a condenser and a pump. There are four different processes in ORC system; pumping, isobaric heat absorption, expansion and isobaric condensation processes. (Zhang et al. 2018, 1209.)

The ORC system shown in figure 2.6 is a single-pressure system without and with the recuperator. If the system is a double pressure system, there are six components in the process. These are a high-pressure evaporator, a low-pressure evaporator, a double-pressure turbine, a recuperator, a condenser and a generator. Exhaust gas from the gas turbines is sent to the evaporators, where the working fluid is heated in evaporators, turning into vapor. Vapor flows to the turbine creating mechanical energy which is transformed to electrical power in a generator. Exhaust of the turbine flows to recuperator. (Sun et al. 2018, 2.) This process can be seen in figure 2.7.

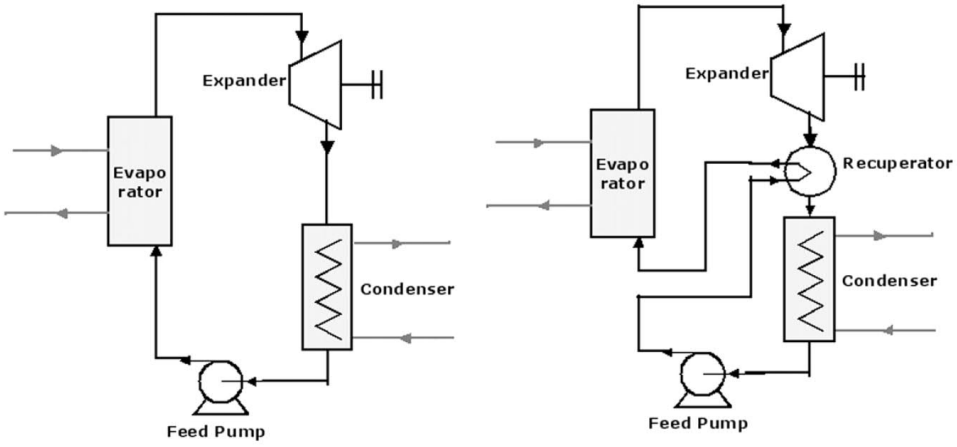

Figure 2.6: ORC system schematic without (left) and with (right) recuperator (Quoilin et al. 2013, 170.)

ORC-systems presented in figure 2.6 can generate electricity or mechanical energy in the expander. If the generated energy is in mechanical form, the expander shaft is connected directly to the driving belt of the engine. There is one drawback in this configuration: the imposed expander speed, that creates a same fixed engine speed. The speed of the turbine might not be the most efficient speed of the engine. (Quoilin et al. 2013, 173.)

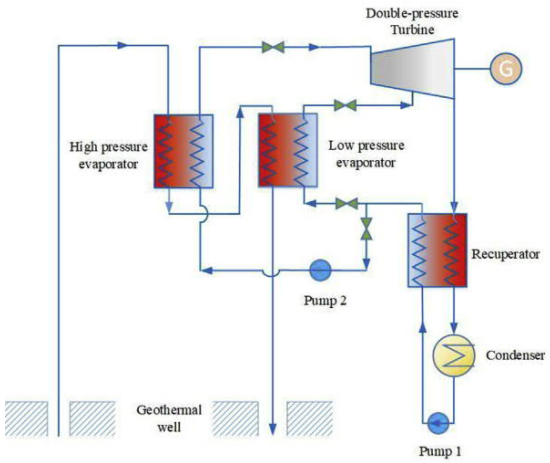

Figure 2.7: Double-pressure ORC system (Sun et al. 2018, 2.)

In organic Rankine cycle the used fluids can be classified to three different categories due to the slopes of their saturation vapor curve in T-s diagram. If the slope is negative, fluids are called “wet fluids”. If the slope is positive, fluids are dry fluids and if the curve is nearly infinitive, fluids are called “isentropic fluids”. Most of the fluids are highly flammable and therefore the diathermic oil circuit between the heat source and the fluid is needed to prevent explosion. (Carcasci et al. 2014, 92.) The T-s diagram of the ORC -process for working fluid R12 can be seen in figure 2.8.

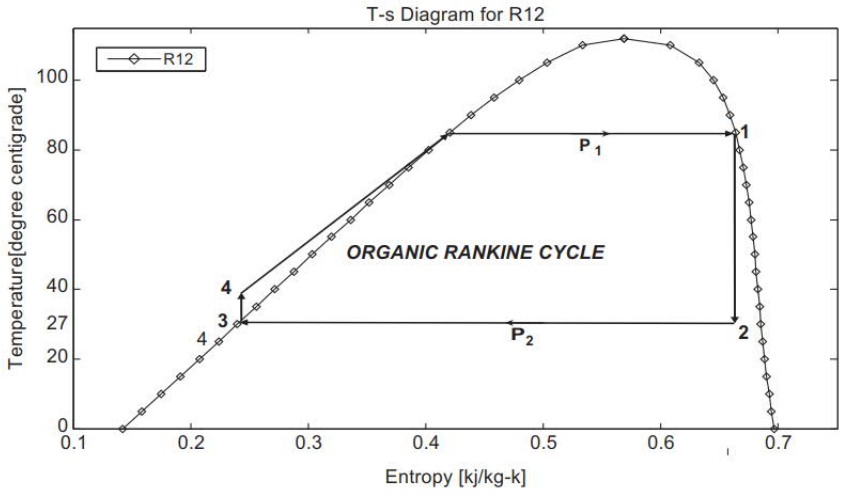

Figure 2.8: Organic Rankine Cycle in T-s diagram with working fluid R-12 (Roy et al. 2010, 5051.)

When low temperature exhaust gases are recovered, the conclusion is that the isentropic fluids are the most suitable. The most important characteristic, for the chosen fluid efficiency, work output and applicability, is the slope in T-s diagram. If the wet fluid is used, it can cause droplets in the last phases of the turbine. Therefore, with wet fluids superheating is needed. When the isentropic fluids are used the vapor stays saturated during expansion and therefore there are no droplets. (Roy et al. 2010, 5049-5050.)

3 HEAT TRANSFER OF FINNED TUBES

In Heat Recovery Steam Generator heat transfer occurs mainly by convection. Because the convection is more efficient on the water side of the tube than on the exhaust gas side, fins are used only on the exhaust gas side. (Kehlhofer et al. 2009, 189.) Finned tube is also called an extended surface in heat transfer. With extended surfaces the direction of heat transfer from boundaries is not the same as the main direction of the heat transfer in the solid material. Extended surfaces increase the effective surface of heat transfer. The material of the fin affects the temperature distribution in the fin, which in turn affects the heat transfer rate. It is not obvious that the heat transfer rate increases when extended surfaces are used. The temperature difference from the base to the tip should be as small as possible making sure the thermal conductivity is as large as possible.

Different types of fins can be seen in the following figure 3.1. An extended surface that is attached to plane wall is called a straight fin (a-b). Fin's distance x from the wall and the cross section can vary with this fin type. The annular fin (c) is a circular plate attached to the cylinder-shaped tube and the cross section of the finned tube varies with the radius from the cylinder wall. For fin types with rectangular cross sections, width and thickness can vary. For circular fins the varying component is $2\pi r$ which is the circumference of the fin. The cross section can be extended, and this is called as pin fin or spine (d). (Incropera et al. 2011, 156-158.)

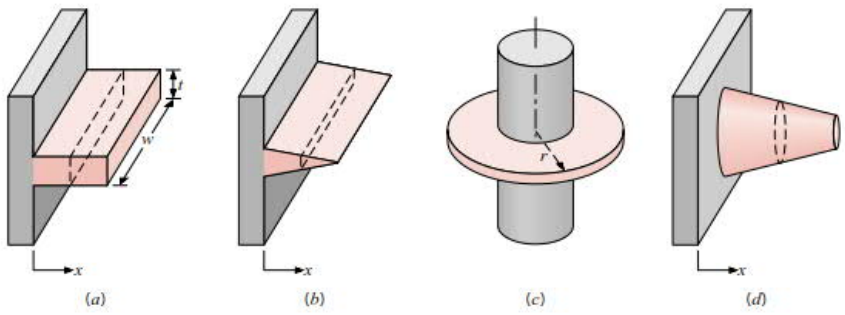

Figure 3.1: Types of fins a) Straight fin of uniform cross section, b) Straight fin of nonuniform section, c) Annular fin and d) Pin fin (Incropera et al. 2011, 156.)

To understand calculation of the fin tubes, heat transfer in one-dimensional and steady state conditions must be described. In this state the heat transfer happens only to one direction. In steady state condition the temperature in each point is independent of time. (Incropera et al. 2011, 112.)

3.1 Heat transfer and temperature distribution in the plane wall

Plane wall separates two different temperature fluids. Heat transfers to direction of coordinate *x* from the hot fluid by convection to surface wall and by conduction through the wall. On the cold side the heat transfers by convection from the surface of the wall to the cold fluid. Boundary conditions of the heat equations reflect to temperature distribution. (Incropera et al. 2011, 112.)

$$\frac{d}{dx}\left(k\frac{dT}{dx}\right) = 0 \tag{3.1.1}$$

where	k	thermal conductivity	[W/mK]
	dx	difference of the distance	[m]
	dT	difference of the temperature	[K]

Heat equation can be defined with equation (3.1.1). The heat transfer can be assumed to be one-dimensional, steady state conditions apply, there is no heat generation and the heat flux is constant. When the thermal conduction is assumed to be constant, the determination of the general solution can start.

$$T(x) = C_1 x + C_2 \tag{3.1.2}$$

where	x	distance	[m]
	C_1	constant 1	[-]
	C_2	constant 2	[-]

When the distance x is assumed to be 0, temperature in this state is marked to be $T_{s,1}$ and when the distance is L, temperature is marked to be $T_{s,2}$. Equation (3.1.2) is a general solution and when the result from distance being zero is added, it generates the form:

$$T_{s,1} = C_2 \tag{3.1.3}$$

Constant 2 is defined in the equation (3.1.3). And when the distance L is added to equation 3.1.2 the general solution becomes:

$$T_{s,2} = C_1 L + C_2 = C_1 L + T_{s,1} \tag{3.1.4}$$

where L total distance [m]

Constant C_1 can be solved from the equation (3.1.4).

$$C_1 = \frac{T_{s,2} - T_{s,1}}{L}$$

The temperature distribution is added to the general solution.

$$T(x) = \left(T_{s,2} - T_{s,1}\right)\frac{x}{L} + T_{s,1} \tag{3.1.5}$$

General solution with temperature distribution can be determined with equation (3.1.5). Heat transfer rate q_x is determined using Fourier's law.

$$q_x = -kA\frac{dT}{dx} = \frac{kA}{L}\left(T_{s,1} - T_{s,2}\right) \tag{3.1.6}$$

where A surface area [m^2]

The heat flux can be solved by integrating the heat transfer rate through x. The heat transfer rate is calculated with equation (3.1.6).

$$q_x'' = \frac{q_x}{A} = \frac{k}{L}\left(T_{s,1} - T_{s,2}\right) \tag{3.1.7}$$

where q_x'' heat flux [W/m^2]

After the heat flux is defined with equation (3.1.7), thermal resistance can be connected to heat conduction. The thermal resistance for conduction in the plane wall is solved.

$$R_{\mathrm{t,cond}} = \frac{T_{\mathrm{s},1} - T_{\mathrm{s},2}}{q_{\mathrm{x}}} = \frac{L}{kA} \tag{3.1.8}$$

where $R_{\mathrm{t,cond}}$ thermal resistance for conduction [W/(m^{2}K)]

Conduction heat transfer can associate to thermal resistance. Thermal resistance for conduction is calculated with equation (3.1.8). Newton's law for cooling is presented.

$$q = hA(T_{\mathrm{s}} - T_{\infty}) \tag{3.1.9}$$

where h heat transfer coefficient [W/(m^{2}K)]

T_{∞} fluid temperature [K]

Thermal resistance for convection can be solved based on the Newton's law for cooling which is presented in equation (3.1.9).

$$R_{\mathrm{t,conv}} = \frac{T_{\mathrm{s}} - T_{\infty}}{q} = \frac{1}{hA} \tag{3.1.10}$$

where $R_{\mathrm{t,conv}}$ thermal resistance for convection [W/(m^{2}K)]

Thermal resistance for convection is calculated with equation (3.1.10). Heat transfer rate can be solved with all the separate elements of the equivalent thermal circuit.

$$q_{\mathrm{x}} = \frac{T_{\infty,1} - T_{\mathrm{s},1}}{1/h_1 A} = \frac{T_{\mathrm{s},1} - T_{\mathrm{s},2}}{L/kA} = \frac{T_{\mathrm{s},2} - T_{\infty,2}}{1/h_2 A} \tag{3.1.11}$$

Heat transfer rate with separate elements can be solved with equation (3.1.11).

Because the resistances are in series, convection and conduction resistances can be summed together.

$$R_{\mathrm{tot}} = \frac{1}{h_1 A} + \frac{L}{kA} + \frac{1}{h_2 A} \tag{3.1.12}$$

With the total thermal resistance R_{tot} and overall temperature difference $T_{\infty,1}$-$T_{\infty,2}$ the heat transfer rate can be determined. Total thermal resistance can be solved with equation (3.1.12).

$$q_x = \frac{T_{\infty,1} - T_{\infty,2}}{R_{tot}} \tag{3.1.13}$$

where $T_{\infty,1}$-$T_{\infty,2}$ overall temperature difference [K]

R_{tot} Total thermal resistance [W/(m^{2}K)]

Heat transfer rate is determined with equation (3.1.13). In the following figure 3.2 the heat transfer through the wall with equivalent thermal circuit can be seen. Also, the temperature distribution is shown in the same figure.

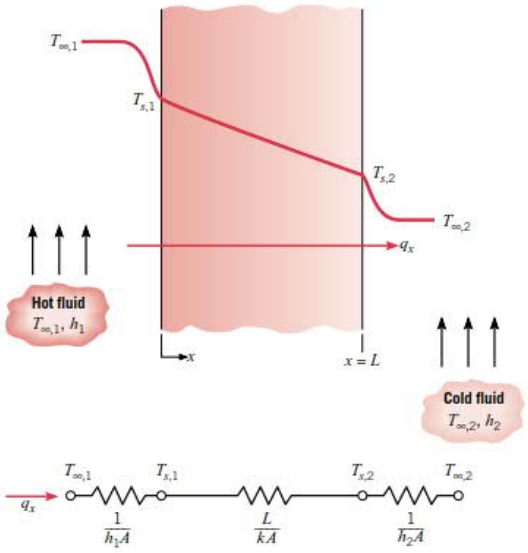

Figure 3.2: Heat transfer through the plane wall with equivalent thermal circuit (Incropera et al. 2011, 113.)

The convection from the hot fluid temperature $T_{\infty,1}$ to surface temperature $T_{s,1}$ is shown in figure 3.2. Furthermore, the conduction from the hot fluid side surface to cold fluid side surface $T_{s,2}$ and convection from the cold surface to cold fluid temperature $T_{\infty,2}$ can be seen from the same figure.

When the convection coefficient is small, the radiation between surface and surroundings must be taken into account.

$$R_{\mathrm{t,rad}} = \frac{T_{\mathrm{s}} - T_{\mathrm{sur}}}{q_{\mathrm{rad}}} = \frac{1}{h_{\mathrm{r}} A} \tag{3.1.14}$$

Radiation between a surface and its surroundings can be solved with equation (3.1.14). Temperature drop between to surface materials is called thermal contact resistance.

$$R''_{\mathrm{t,c}} = \frac{T_{\mathrm{A}} - T_{\mathrm{B}}}{q''_{\mathrm{x}}} \tag{3.1.15}$$

where	$R''_{\mathrm{t,c}}$	thermal contact resistance	[W/(m^{2}K)]
	T_{A}	temperature in material A	[K]
	T_{B}	temperature in material B	[K]

In the following figure 3.3 the thermal contact resistance between two different materials is shown, and it can be calculated with equation (3.1.15).

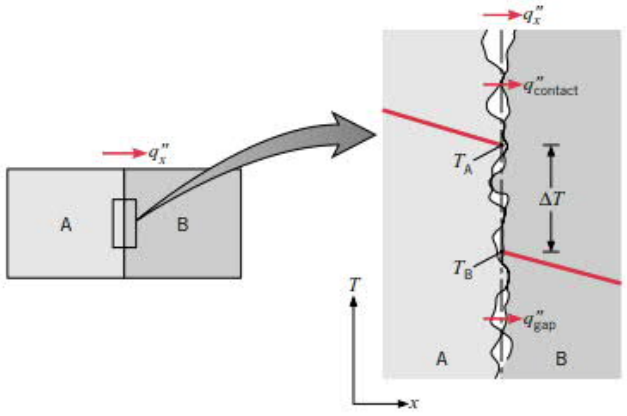

Figure 3.3: Temperature difference and thermal contact resistance between two materials A and B (Incropera et al. 2011, 118.)

This temperature difference is due the roughness of the surfaces of the different materials illustrated in figure 3.3. Gaps between contact spots are filled with air and the heat transfers as conduction in contact spots and as convection and radiation in the gaps. The contact

resistance can be calculated as two parallel resistances, the one in gaps and the one in contact spots. If the surface is rough, most of the heat transfer happens through the gaps. (Incropera et al. 2011, 118.)

3.2 Conduction in cylinder that can be assumed as a pipe

Cylindrical shaped objects are commonly assumed to be hollow in heat transfer calculations. Hot fluid flows inside the cylinder and cold fluid on the outside. (Incropera et al. 2011, 136.) When the condition is steady state and there is no heat generation.

$$\frac{1}{r}\frac{d}{dr}\left(kr\frac{dT}{dr}\right) = 0 \qquad (3.2.1)$$

where r radius [m]

Heat equation when there is no heat generation can be defined with equation (3.2.1). Thermal conductivity k can be treated as a variable (Incropera et al. 2011, 136.) Heat transfer in a hollow cylinder can be seen in the following figure 3.4.

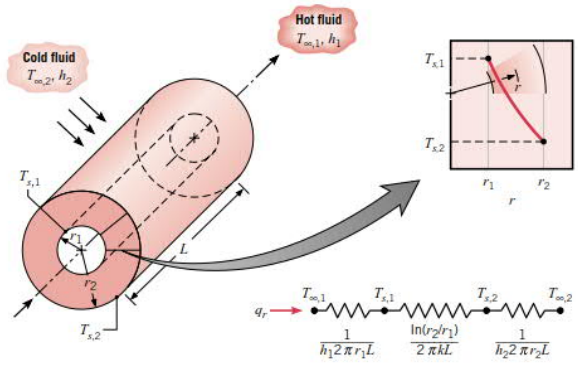

Figure 3.4: Heat transfer in hollow cylinder (Incropera et al. 2009, 136.)

The convection from the hot fluid temperature $T_{\infty,1}$ to surface temperature $T_{s,1}$ is shown in figure 3.4. Furthermore, the conduction from the hot fluid side surface to cold fluid side surface $T_{s,2}$ and convection from the cold surface to cold fluid temperature $T_{\infty,2}$ can be seen from the same figure.

Heat transfer rate can be calculated with a form of Fourier's law.

$$q_r = -kA\frac{dT}{dr} = -k(2\pi rL)\frac{dT}{dr} \quad (3.2.2)$$

The heat transfer rate is constant to radial direction. Heat transfer rate can be calculated with equation (3.2.2). When the thermal conduction is assumed to be constant the general solution can be defined.

$$T(r) = C_1 \ln r + C_2 \quad (3.2.3)$$

When the radius is r_1 the temperature is determined as $T_{s,1}$ and when the radius is r_2 the temperature is $T_{s,2}$. When these are added to general solution (3.2.3), the temperature $T_{s,1}$ can be solved.

$$T_{s,1} = C_1 \ln r_1 + C_2 \quad (3.2.4)$$

Temperature $T_{s,1}$ can be defined with equation (3.2.4) and temperature $T_{s,2}$ can be also solved.

$$T_{s,2} = C_1 \ln r_2 + C_2 \quad (3.2.5)$$

Temperature $T_{s,2}$ can be calculated with equation (3.2.5). The C_1 and C_2 are added to general solution (3.2.3). Temperature at a certain radius can be calculated.

$$T(r) = \frac{T_{s,1}-T_{s,2}}{\ln(r_1/r_2)} \ln\left(\frac{r}{r_2}\right) + T_{s,2} \quad (3.2.6)$$

Temperature distribution in radial conduction through the cylinder wall is logarithmic. (Incropera et al. 2011, 137). Temperature for a radius can be defined with equation (3.2.6). Heat transfer rate can be solved.

$$q_r = \frac{2\pi Lk(T_{s,1}-T_{s,2})}{\ln(r_2/r_1)} \quad (3.2.7)$$

Heat transfer rate can be calculated with equation (3.2.7). Thermal resistance of the heat transfer through the cylinder wall can be calculated.

$$R_{t,cond} = \frac{\ln(r_2/r_1)}{2\pi Lk} \quad (3.2.8)$$

Thermal resistance of the heat transfer through cylinder can be calculated with equation (3.2.8).

3.3 Finned tubes in conduction

Conduction in finned tubes can be simplified if some assumptions are made. Conduction with fins is two dimensional, but the assumption is made that the situation is one dimensional to a longitudinal direction. It is also assumed that the temperature is the same across the whole cross-sectional area. Also, conditions are assumed to be in a steady-state and that the thermal conductivity is constant. Furthermore, the convection heat transfer coefficient is the same over the entire surface. (Incropera et al. 2011, 157) Energy balance in the fin can be seen in following figure 3.5.

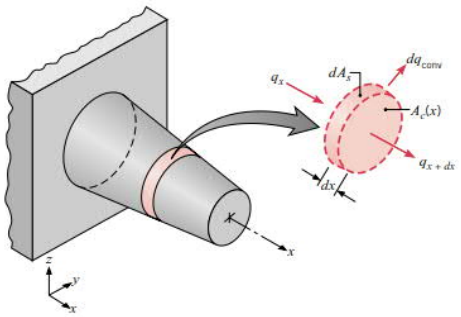

Figure 3.5: Energy balance for a fin structure (Incropera et al. 2011, 157.)

Conduction heat rate q_x at x can be calculated.

$$q_x = q_{x+dx} + dq_{conv} \tag{3.3.1}$$

where q_{x+dx} conduction heat rate at x+dx [-]

dq_{conv} convection heat transfer rate [-]

Conduction heat rate can be defined with equation (3.3.1) and it can be also determined with Fourier's law.

$$q_x = -kA_{cross}\frac{dT}{dx} \tag{3.3.2}$$

where A_{cross} cross-sectional area [m^2]

Conduction heat rate at x, can be calculated with equation (3.3.2). Conduction heat rate q_{x+dx} at x+dx can be calculated.

$$q_{x+dx} = q_x + \frac{dq_x}{dx} dx \tag{3.3.3}$$

Conduction heat rate at x+dx can be solved with equation (3.3.3) and it can also be expressed in another way.

$$q_{x+dx} = -kA_{cross} \frac{dT}{dx} - k \frac{d}{dx}\left(A_{cross} \frac{dT}{dx}\right) dx \tag{3.3.4}$$

Conduction heat transfer rate at x+dx is calculated with equation (3.3.4). Convection heat transfer rate with a differential surface area is defined.

$$dq_{conv} = hdA_s(T - T_\infty) \tag{3.3.5}$$

where

h	heat transfer coefficient	[W/(m^{2}K)]
dA_s	differential element surface area	[m^2]
T	temperature of the surface	[K]
T_∞	fluid temperature	[K]

Equations (3.3.1) - (3.3.5) can be converted into an energy balance for the fin.

$$\frac{d}{dx}\left(A_{cross} \frac{dT}{dx}\right) - \frac{h}{k} \frac{dA_s}{dx} (T - T_\infty) = 0 \tag{3.3.6}$$

To solve equation (3.3.6) we need to be more specific about geometry. It is assumed that fins are attached to base surface of temperature $T(0) = T_b$ and extends to T_∞. Cross-sectional area A_c is assumed to be constant and the surface area A_s is fin perimeter P multiplied with distance of the fin x. Now the equation (3.3.6) can be reduced.

$$\frac{d^2T}{dx^2} - \frac{hP}{kA_{cross}} (T - T_\infty) = 0 \tag{3.3.7}$$

To simplify equation (3.3.7) temperature difference is transformed to excess temperature θ.

$$\theta(x) \equiv T(x) - T_\infty \tag{3.3.8}$$

where $T(x)$ temperature at x [K]

Because the fluid temperature T_∞ is constant, the equation (3.3.8) can be transferred to a form.

$$\frac{d^2\theta}{dx^2} - m^2\theta = 0 \tag{3.3.9}$$

where $m^2 \equiv \frac{hP}{kA_{\text{cross}}}$

Energy balance when the fluid temperature is constant, can be determined with equation (3.3.9). Because the effective surface area is increasing when the fins are used, the heat transfer from the surface is also increasing. It is not clear that the heat transfer is increasing when the number of fins is increasing. This can be evaluated with fin effectiveness ε_{fin}. (Incropera et al. 2011, 164.)

$$\varepsilon_{\text{fin}} = \frac{q_{\text{fin}}}{hA_{\text{cross,b}}\theta_{\text{b}}} \tag{3.3.10}$$

where $A_{\text{cross,b}}$ fin cross-sectional are at the base [m^2]

q_{fin} conduction heat rate at the fin [W]

Fin effectiveness should be as high as possible, and the fins are not used if the effectiveness is less than equal to two $\varepsilon_f \leq 2$. Fin effectiveness can be calculated with equation (3.3.10). Fin effectiveness can also be calculated in another way.

$$\varepsilon_{\text{fin}} = \left(\frac{kP}{hA_{\text{cross}}}\right)^{1/2} \tag{3.3.11}$$

Fin effectiveness can also be defined with equation (3.3.11). One value that relates to fin effectiveness is the high thermal conductivity of the material. The material should be chosen to be aluminum alloys or copper. The thermal conductivity of copper is higher than that of aluminum, but aluminum alloys are lighter and cheaper than copper. Fin effectiveness is higher also when the ratio of perimeter to cross-sectional area of the fins is larger. Therefore,

it is more effective to use thin fins with small spaces between them. Fin gap should not be reduced too much because then the convection coefficient is reducing. (Incropera et al. 2011, 164.)

There is more need for extended surfaces with gaseous fluids and when the heat transfer is natural convection. In the case where the fins are used in a gas/ liquid heat transfer, they are located on the gas side where the convection coefficient is lower. One part of fin performance is the thermal resistance. (Incropera et al. 2011, 165.) Thermal resistance within fins can be defined.

$$R_{\mathrm{t,fin}} = \frac{\theta_{\mathrm{b}}}{q_{\mathrm{fin}}} \tag{3.3.12}$$

Thermal resistance within fins is calculated with equation (3.3.12). Thermal resistance at the base of the fin can be calculated.

$$R_{\mathrm{t,b}} = \frac{1}{hA_{\mathrm{cross,b}}} \tag{3.3.13}$$

Thermal resistance at the base of the fin is defined with equation (3.3.13). Fin effectiveness can also be defined with thermal resistances of the fin and its base. This can be seen as a conversion of equation (3.3.10).

$$\varepsilon_{\mathrm{fin}} = \frac{R_{\mathrm{t,b}}}{R_{\mathrm{t,fin}}} \tag{3.3.14}$$

Fin effectiveness can be increased by reducing convection/conduction resistance. Fin effectiveness can be calculated with equation (3.3.14). The thermal performance of the fin can be measured also with fin efficiency η_{f}. The most important value for thermal performance is the temperature difference between the base of the fin and the fluid. If the whole fin would be in the temperature of the base, the efficiency would be highest. Fin efficiency can be defined.

$$\eta_{\mathrm{fin}} \equiv \frac{q_{\mathrm{fin}}}{q_{\mathrm{max}}} = \frac{q_{\mathrm{fin}}}{hA_{\mathrm{fin}}\theta_{\mathrm{b}}} \tag{3.3.15}$$

where A_{fin} surface area of the fin [m^2]

Fin efficiency is calculated with equation (3.3.15).

3.4 Overall Surface Efficiency

Overall surface efficiency η_o is a characteristic of the whole array of fins, including the base surface where the fins are attached (Incropera et al. 2011, 153).

$$\eta_o = \frac{q_{tot}}{q_{max}} = \frac{q_{tot}}{hA_{tot}\theta_b} \quad (3.4.1)$$

where q_{tot} total heat rate [W]

A_{tot} total surface area [m^2]

Overall surface efficiency can be calculated with equation (3.4.1). Total surface area can be calculated with surface area of one fin and surface area of the base.

$$A_{tot} = N_{fin}A_{fin} + A_b \quad (3.4.2)$$

where N_{fin} number of fins [-]

A_b surface area of the base [m^2]

Total surface area can be calculated with equation (3.4.2). Equation (3.4.1) can be transferred to a different form.

$$\eta_o = 1 - \frac{NA_{fin}}{A_{tot}}(1 - \eta_{fin}) \quad (3.4.3)$$

The total heat rate can be calculated from equation (3.4.1) when the overall efficiency is known. Also, overall thermal resistance $R_{t,o}$ can be calculated when the overall efficiency is known from equation (3.4.3.)

$$R_{t,o} = \frac{\theta_b}{q_{tot}} = \frac{1}{\eta_o hA_{tot}} \quad (3.4.4)$$

Overall thermal resistance accounts for parallel heat flow paths by convection and conduction that occur in fins, and by convection from the surface. Overall thermal resistance

can be solved with equation (3.4.4). The thermal contact resistance $R_{t,c}$ affects the overall thermal performance.

$$R_{t,o(c)} = \frac{\theta_b}{q_{tot}} = \frac{1}{\eta_{o(c)} h A_{tot}} \tag{3.4.5}$$

Corresponding to equation (3.4.5) the overall surface efficiency can be calculated.

$$\eta_{o(c)} = 1 - \frac{N A_{fin}}{A_{tot}} \left(1 - \frac{\eta_{fin}}{C_1}\right) \tag{3.4.6}$$

where $$C_1 = 1 + \eta_{fin} h A_{fin} \left(\frac{R''_{t,c}}{A_{cross,b}}\right)$$

Overall surface efficiency can be calculated with equation (3.4.6).

3.5 External flow of the tubes and tube banks

Tubes can be assumed to be a cylinder in a cross flow. The free stream of fluid comes to *a forward stagnation point* demonstrated in figure 3.6. In this phase the pressure increases. After this point the pressure decreases as the *x* increases. Because the adverse pressure gradient is larger than zero, the *boundary layer* is formed. Behind the cylinder, the fluid lacks enough momentum to overcome the pressure gradient and therefore *boundary layer separation* occurs. Reynolds number is one of the most relevant factors of the occurrence of the boundary layer transition. (Incropera et al. 2011, 455.)

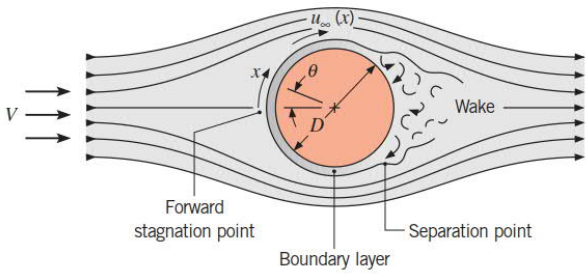

Figure 3.6: Boundary formation and separation in case of circular cylinder in a cross flow (Incropera et al. 2011, 455.)

The Reynolds number can be defined.

$$Re_D = \frac{\rho V D}{\mu} = \frac{VD}{v} \tag{3.5.1}$$

where			
	Re_D	Reynold number	[-]
	ρ	density	[kg/m^3]
	V	velocity of the fluid	[m/s]
	μ	dynamic viscosity	[Ns/m^2]
	v	kinematic viscosity	[m^2/s]

When the Reynolds number is calculated with the equation (3.5.1) the Nusselt number can be defined. To solve the value of the Nusselt number also the Prandtl number has to be known. Nusselt number can be calculated with numerous scenario-specific correlations. (Incropera et al. 2011, 458.) Nusselt number can be defined with Hilpert correlation.

$$\overline{Nu_D} = \frac{\bar{h}D}{k} = CRe_D^m Pr^{1/3} \tag{3.5.2}$$

where			
	Nu_D	Nusselt number	[-]
	m	constant 1	[-]
	C	constant 2	[-]
	Pr	Prandtl number	[-]

Hilpert correlation is used when Pr>0.7 and constants C and m are from table 3.1. Hilpert correlation can be defined with equation (3.5.2).

Table 3.1: Constants of the equation 3.5.2 (Incropera et al. 2011, 458.)

Re_D	C	m
0,4 - 4	0,989	0,330
4 - 40	0,911	0,385
40 - 4 000	0,683	0,466
4 000 - 40 000	0,193	0,618
40 000 - 400 000	0,027	0,805

Also, correlation of Zukauskas is recommended calculating a cylinder in the cross flow. Prandtl number should be $0.7 < Pr < 500$ and Reynolds number $1 < Re_D < 10^6$. Nusselt number can be defined with Zukauskas.

$$\overline{Nu_D} = CRe_D^m Pr^n \left(\frac{Pr}{Pr_s}\right)^{1/4} \quad (3.5.3)$$

where Pr_s Prandtl number at T_s [-]

n constant 3 [-]

Correlation of Zukauskas can be determined with equation (3.5.3). If the Prandtl number is $Pr<10$ the constant n is 0.37 and if the Prandtl is $Pr>10$ the constant n is 0.36. Constants C and m can be seen in table 3.2.

Table 3.2: Constant of the equation 3.5.3 (Incropera et al. 2011, 459).

Re_D	C	m
1 - 40	0,75	0,4
40 - 1000	0,51	0,5
10^3 - 2 x 10^5	0,26	0,6
2 x 10^5 - 10^6	0,076	0,7

Correlation of Churchill and Bernstein is supposed to cover the entire range of the Reynolds number as well as a wide range of Prandtl numbers. Prandtl number should be under 0.2 when this correlation is used. (Incropera et al. 2011, 458.)

$$\overline{Nu_D} = 0.3 + \frac{0.62 Re_D^{1/2} Pr^{1/3}}{\left[1+(0.4/Pr)^{2/3}\right]^{1/4}} \left[1 + \left(\frac{Re_D}{282000}\right)^{5/8}\right]^{4/5} \quad (3.5.4)$$

Correlation of Churchill and Bernstein can be defined with equation (3.5.4). In case of heat exchangers and heating coils, the bank of tubes on cross flow is the main calculation factor. Tube rows in the bank can be aligned or staggered. Distance of the tubes can be defined with transverse pitch S_T and longitudinal pitch S_L which are measured from tube centerlines. (Incropera et al. 2011, 468.) This can be seen in figure 3.7.

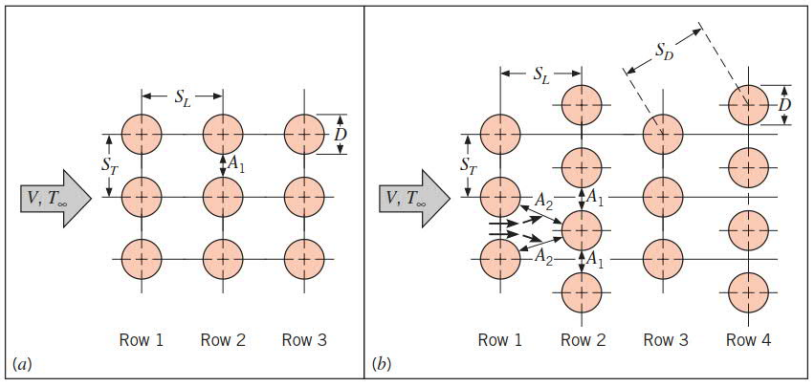

Figure 3.7: Tube bank arrangements (a) aligned and (b) staggered (Incropera et al. 2011, 469.)

The flow around the tubes on the first row is similar to a single cylinder in the cross flow. In an aligned arrangement the convection coefficient increases with increasing row number. If the relation between transverse pitch and longitudinal pitch is $S_T/S_L < 0.7$, then the aligned arrangement should not be used. Normally it is considered good to know the average heat transfer coefficient for the whole tube bank. Nusselt number can be defined with correlation of Zukauskas for different tube arrangements. Number of tube rows should be $N_L > 20$, Prandtl number should be $0.7 < Pr < 500$ and maximum Reynolds number should be $10 < Re_{D,max} < 2 \cdot 10^6$ if this correlation is used. (Incropera et al. 2011, 469)

$$\overline{Nu_D} = C_1 Re_{D,max}^m Pr^{0.36} \left(\frac{Pr}{Pr_s}\right)^{1/4} \quad (3.5.5)$$

Correlation of Zukauskas for different tube arrangements is determined with equation (3.5.5). Constants C_1 and m can be chosen from in table 3.3.

Table 3.3: Constants of the equation 3.5.5 (Incropera et al. 2011, 470.)

Arrangement	***Re_D***	***C***	***m***
Aligned	$10 - 10^2$	0,80	0,40
Staggered	$10 - 10^2$	0,90	0,40
Aligned	$10^2 - 10^3$	Appromately as a single	
Staggered	$10^2 - 10^3$	(isolated) cylinder	
Aligned ($S_T/S_L > 0,7$)	$10^3 - 2 \times 10^5$	0,27	0,63
Staggered ($S_T/S_L < 2$)	$10^3 - 2 \times 10^5$	$0,35(S_T/S_L)^{1/5}$	0,60
Staggered ($S_T/S_L > 2$)	$10^3 - 2 \times 10^5$	0,40	0,60
Aligned	$2 \times 10^5 - 2 \times 10^6$	0,021	0,84
Staggered	$2 \times 10^5 - 2 \times 10^6$	0,022	0,84

Because the temperature changes a lot as the fluid moves through tube bank, the temperature difference should be calculated with log-mean temperature difference method. (Incropera et al. 2011, 472.)

$$\Delta T_{lm} = \frac{(T_s - T_i) - (T_s - T_o)}{\ln\left(\frac{T_s - T_i}{T_s - T_o}\right)} \tag{3.5.6}$$

where ΔT_{lm} log-mean temperature difference [K]

T_s surface temperature [K]

T_i bank inlet temperature [K]

T_o bank outlet temperature [K]

Log mean temperature difference can be calculated with equation (3.5.6). The bank outlet temperature can be determined.

$$\frac{T_s - T_o}{T_s - T_i} = \exp\left(\frac{\pi D N_{\mathrm{tot,T}} \bar{h}}{\rho V N_T S_T c_p}\right) \quad (3.5.7)$$

where $N_{\mathrm{tot,T}}$ total number of the tubes [-]

N_{T} number of tubes in each row [-]

Bank outlet determination can be defined with equation (3.5.7). When the temperature difference is calculated, the heat transfer rate per length unit can be defined.

$$q' = N_{\mathrm{tot,T}}\left(\bar{h}\pi D \Delta T_{\mathrm{lm}}\right) \quad (3.5.8)$$

Heat transfer rate per length unit can be calculated with equation (3.5.8).

3.6 NTU-method

When the inlet temperature of the fluid is known and the outlet parameters can be defined or are already known, the LMTD method can be used. When just the fluid inlet temperature is defined the alternative solution, effectiveness-NTU, should be used. (Incropera et al. 2011, 722.)

Maximum possible heat transfer rate has to be solved first to define effectiveness of a heat exchanger.

$$q_{\max} = C_{\min}\left(T_{\mathrm{h,i}} - T_{\mathrm{c,i}}\right) \quad (3.6.1)$$

where $q_{\max}$ maximum heat transfer rate [W]

$C_{\min}$ minimum heat capacity rate [J/K]

$T_{\mathrm{h,i}}$ hot fluid inlet temperature [K]

$T_{\mathrm{c,i}}$ cold fluid inlet temperature [K]

Minimum heat capacity rate is the smaller one from the hot fluid heat capacity rate and cold fluid heat capacity rate. Now the effectiveness can be defined as a ratio between the available heat transfer rate and the maximum value of heat transfer rate.

With equation (3.6.1) the maximum value of heat transfer rate is calculated. (Incropera et al. 2011, 722.)

$$\varepsilon \equiv \frac{q}{q_{\max}} \tag{3.6.2}$$

where ε effectiveness [-]

Actual heat transfer rate q can be defined after the effectiveness is calculated with equation (3.6.2).

$$q = \varepsilon C_{\min}\left(T_{\mathrm{h,i}} - T_{\mathrm{c,i}}\right) \tag{3.6.3}$$

Actual heat rate can be solved with equation (3.6.3). Number of heat transfer units (NTU) is a dimensionless parameter.

$$NTU \equiv \frac{UA}{C_{\min}} \tag{3.6.4}$$

where NTU number of heat transfer units [-]

U overall heat transfer coefficient [W/m^{2}K]

A area [m^2]

Number of heat transfer units can be determined with equation (3.6.4). For different type of heat exchangers there are different heat exchanger effectiveness relations. For a parallel flow heat exchanger, the effectiveness is defined.

$$\varepsilon = \frac{1-\exp[-NTU(1+C_{\mathrm{r}})]}{1+C_{\mathrm{r}}} \tag{3.6.5}$$

where C_{r} heat capacity ratio [-]

Effectiveness for parallel flow heat exchanger is calculated with equation (3.6.5). Heat capacity ratio is a ratio between minimum and maximum heat capacities. For a counterflow heat exchanger, the effectiveness can be calculated when the heat capacity ratio is below one ($C_{\mathrm{r}} < 1$).

$$\varepsilon = \frac{1-\exp[-NTU(1-C_r)]}{1-C_r\exp[-NTU(1-C_r)]} \tag{3.6.6}$$

When the heat capacity ratio is below one, effectiveness can be calculated with equation (3.6.6). When the heat capacity ratio is one (C_r = 1), the effectiveness is defined.

$$\varepsilon = \frac{NTU}{1+NTU} \tag{3.6.7}$$

Effectiveness when the heat capacity is one, can be solved with equation (3.6.7). For shell-and-tube heat exchanger with one shell pass the effectiveness can be calculated.

$$\varepsilon_1 = 2 \cdot \left\{1 + C_r + (1 + C_r^2)^{1/2} \cdot \frac{1+\exp\left[-NTU\cdot\left(1+C_r^2\right)^{1/2}\right]}{1-\exp\left[-NTU\cdot\left(1+C_r^2\right)^{1/2}\right]}\right\}^{-1} \tag{3.6.8}$$

where ε_1 effectiveness for one shell pass [-]

For shell-and-tube heat exchanger with one shell pass the effectiveness can be defined with equation (3.6.8). If there are more than one shell pass, the effectiveness can be defined.

$$\varepsilon = \left[\left(\frac{1-\varepsilon_1 C_r}{1-\varepsilon_1}\right)^n\right]\left[\left(\frac{1-\varepsilon_1 C_r}{1-\varepsilon_1}\right)^n - C_r\right]^{-1} \tag{3.6.9}$$

where n number of shell passes [-]

Effectiveness for shell-and-tube heat exchanger with more than one shell pass, can be calculated with equation (3.6.9). For single pass cross-flow heat exchanger, the effectiveness can be defined when both fluids are mixed.

$$\varepsilon = 1 - \exp\left[\left(\frac{1}{C_r}\right)(NTU)^{0,22}\{\exp[-C_r(NTU)^{0,78}] - 1\}\right] \tag{3.6.10}$$

Effectiveness for single cross-flow heat exchanger when the both flows are mixed, can be solved with equation (3.6.10). If fluid with maximum heat capacity is mixed and fluid with minimum heat capacity is unmixed, the effectiveness can be calculated.

$$\varepsilon = \left(\frac{1}{C_r}\right)(1 - \exp\{-C_r[1 - \exp(-NTU)]\}) \tag{3.6.11}$$

Effectiveness can be defined also with equation (3.6.11). If fluid with minimum heat capacity is mixed and fluid with maximum heat capacity is unmixed, the effectiveness can be solved.

$$\varepsilon = 1 - \exp(-C_r^{-1}\{1 - \exp[-C_r(NTU)]\}) \quad (3.6.12)$$

With equation (3.6.12), effectiveness can be determined. For all exchanger types if the heat capacity ratio is zero ($C_r = 0$) the effectiveness can be calculated.

$$\varepsilon = 1 - \exp(-NTU) \quad (3.6.13)$$

If the heat capacity ratio is zero, the effectiveness can be solved with equation (3.6.13). When the effectiveness is calculated also the number of heat transfer units (NTU) can be defined. For a parallel flow the NTU can be defined.

$$NTU = -\frac{\ln[1-\varepsilon(1+C_r)]}{1+C_r} \quad (3.6.14)$$

For a parallel flow heat exchanger, the NTU can be calculated with equation (3.6.14). For a counterflow heat exchanger, the NTU is calculated when the heat capacity ratio is below one ($C_r < 1$).

$$NTU = \frac{1}{C_r-1}\ln\left(\frac{\varepsilon-1}{\varepsilon C_r-1}\right) \quad (3.6.15)$$

Effectiveness for a counterflow heat exchanger the NTU can be defined with equation (3.6.15). When the heat capacity ratio is one ($C_r = 1$), the NTU can be defined with the following equation.

$$NTU = \frac{\varepsilon}{1-\varepsilon} \quad (3.6.16)$$

If the heat capacity ratio is one, the NTU can be solved with equation (3.6.16). For shell-and-tube heat exchanger with one shell pass the NTU can be defined with following equations.

$$(NTU)_1 = -(1 + C_r^2)^{-1/2}\ln\left(\frac{E-1}{E+1}\right) \quad (3.6.17)$$

where $$E = \frac{2/\varepsilon_1 - (1+C_r)}{(1+C_r^2)^{1/2}} \quad (3.6.18)$$

If there is just one shell pass in shell-and-tube heat exchanger, the NTU can be calculated with equations (3.6.17) and (3.6.18). If there are more than one shell pass, the NTU can be calculated with following equations.

$$\varepsilon_1 = \frac{F-1}{F-C_r} \quad (3.6.19)$$

where $$F = \left(\frac{\varepsilon C_r - 1}{\varepsilon - 1}\right)^{1/n} \quad (3.6.20)$$

If there are more than one shell pass, the NTU can be solved with equations (3.6.19) and (3.6.20). For a single pass cross-flow heat exchanger, the NTU can be defined when the fluid with maximum heat capacity is mixed and fluid with minimum heat capacity is unmixed.

$$NTU = -\ln\left[1 + \left(\frac{1}{C_r}\right)\ln(1 - \varepsilon C_r)\right] \quad (3.6.21)$$

For a single pass cross-flow heat exchanger the NTU can be defined with equation (3.6.21). If the fluid with minimum heat capacity is mixed and fluid with maximum heat capacity is unmixed, the NTU can be solved from the following equation.

$$NTU = -\left(\frac{1}{C_r}\right)\ln[C_r \ln(1 - \varepsilon) + 1] \quad (3.6.22)$$

NTU for a cross-flow heat exchanger can be solved with equation (3.6.22). For all exchangers, if the heat capacity ratio is zero ($C_r = 0$) the NTU can be calculated with the following equation.

$$NTU = -\ln(1 - \varepsilon) \quad (3.6.23)$$

When the heat capacity ratio is zero the NTU can be determined with equation (3.6.23).

3.7 LMTD- method

To design an efficient heat exchanger the total heat transfer rate, surface area and heat transfer coefficient have to be determined. These calculations are possible to do based on energy balances. Heat exchanger external heat transfer to surroundings is assumed to be negligible.

$$q = q_{\mathrm{m,h}}\left(H_{\mathrm{h,i}} - H_{\mathrm{h,o}}\right) \tag{3.7.1}$$

Hot fluid steady flow energy balance can be calculated with equation (3.7.1).

$$q = q_{\mathrm{m,c}}\left(H_{\mathrm{c,o}} - H_{\mathrm{c,i}}\right) \tag{3.7.2}$$

For cold fluid steady flow energy balance can be defined with equation (3.7.2). If the constant specific heats (c_{p}) are known, the energy balance for the hot fluid can be solved with the following equation.

$$q = q_{\mathrm{m,h}} c_{\mathrm{p,h}}\left(T_{\mathrm{h,i}} - T_{\mathrm{h,o}}\right) \tag{3.7.3}$$

Energy balance of the hot fluid can be solved with equation (3.7.3) when the constant specific heats are known.

$$q = q_{\mathrm{m,c}} c_{\mathrm{p,c}}\left(T_{\mathrm{c,o}} - T_{\mathrm{c,i}}\right) \tag{3.7.4}$$

For the cold fluid the energy balance with specific heat can be solved with equation (3.7.4). The rate of total heat transfer q can be solved based on the log mean temperature difference ΔT_{lm}, heat transfer area and overall heat transfer coefficient.

$$q = UA\Delta T_{\mathrm{lm}} \tag{3.7.5}$$

Total heat transfer rate can be solved with equation (3.7.5) when the log mean temperature is known.

$$\Delta T_{\mathrm{lm}} = \frac{\Delta T_2 - \Delta T_1}{\ln(\Delta T_2 / \Delta T_1)} = \frac{\Delta T_1 - \Delta T_2}{\ln(\Delta T_1 / \Delta T_2)} \tag{3.7.6}$$

Log mean temperature difference can be calculated with equation (3.7.6). For a parallel-flow heat exchanger temperature differences ΔT_1 and ΔT_2 can be defined as

$$\Delta T_1 \equiv T_{h,1} - T_{c,1} = T_{h,i} - T_{c,i} \text{ and } \Delta T_2 \equiv T_{h,2} - T_{c,2} = T_{h,o} - T_{c,o}.$$

For a counterflow heat exchanger the temperature differences ΔT_1 and ΔT_2 can be solved as

$$\Delta T_1 \equiv T_{h,1} - T_{c,1} = T_{h,i} - T_{c,o} \text{ and } \Delta T_2 \equiv T_{h,2} - T_{c,2} = T_{h,o} - T_{c,i}.$$

3.8 Internal flow in the tubes

Concerning the external flow, one of the main considerations is to know if the flow is laminar or turbulent. This same should be thought with internal flow in tubes. Also, the existence of both entrance and fully developed regions should be researched. When the fluid contacts the wall of the pipe, the viscosity of the fluid develops a boundary layer as the distance from the entrance increases. After there is no inviscid flow region anymore, the whole flow is fully developed. (Incropera et al. 2011, 518.) This can be seen in figure 3.8.

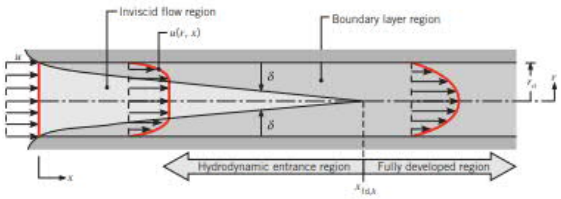

Figure 3.8: Hydrodynamic boundary layer development in circular tube (Incropera et al. 2011, 518.)

The flow is fully developed when the velocity profile is not changing as the distance increases. In a circular tube the fully developed velocity profile is parabolic for laminar flow. If the flow is turbulent, the velocity profile is flatter because the turbulent is mixing. (Incropera et al. 2011, 519.) For internal flow the type of the flow can be defined by calculating the Reynolds number. For a circular tube of a known diameter the Reynolds number can be calculated when the velocity of the flow and viscosities are known.

$$Re_D = \frac{\rho V_m D}{\mu} = \frac{V_m D}{\nu} \tag{3.8.1}$$

If the Reynolds number is below 2300, the flow is laminar. If the Reynolds number for the internal flow is over 2300, the flow can be determined to be turbulent. In the tube the velocity in different locations of the cross-section varies. Therefore, calculations are made with a mean velocity of the internal flow. The mass flow rate can be defined when the density of the fluid and cross-sectional area is known. (Incropera et al. 2011, 519.)

$$q_{\mathrm{m,internal}} = \rho V_{\mathrm{m}} A_{\mathrm{c}} \tag{3.8.2}$$

Pump and fan requirements depend on the pressure drop in the tube. Pressure drop can be defined with the Moody's friction factor. It can be defined as

$$f = \frac{-(dp/dx)D}{\frac{\rho V_{\mathrm{m}}^2}{2}} \tag{3.8.3}$$

where f Moody's friction factor [-]

Friction coefficient which is called also as Fanning friction factor. It can be defined when the Reynolds number is calculated as

$$C_{\mathrm{f}} = \frac{64}{Re_{\mathrm{D}}} \tag{3.8.4}$$

where C_{f} Fanning friction factor [-]

The friction factor indicates tube surface conditions and it increases when the tube wall surface roughness increases. Experimental correlation made by Colebrook for a wide range of conditions can be defined as

$$\frac{1}{\sqrt{f}} = -2{,}0 \log\left[\frac{e/D}{3{,}7} + \frac{2{,}51}{Re_{\mathrm{D}}\sqrt{f}}\right] \tag{3.8.5}$$

where e relative roughness of the surface [-]

For a smooth surface with a large Reynolds number the Petukhov correlation can be used. Reynolds number should be between 3000 - $5 \cdot 10^6$ for this equation to work.

$$f = (0{,}790 \ln Re_D - 1{,}64)^{-2} \tag{3.8.6}$$

The Nusselt number for a fully developed turbulent flow in a smooth tube can be defined for heating when the Reynolds and Prandtl numbers are known with correlation by Dittus-Boelter

$$Nu_D = 0{,}023 Re_D^{4/5} Pr^{0,4} \quad (3.8.7a)$$

And for cooling

$$Nu_D = 0{,}023 Re_D^{4/5} Pr^{0,3} \quad (3.8.7b)$$

These equations (3.8.7a) and (3.8.7b) are valid when the Prandtl number is between 0,6-160, Reynolds number is over 10 000 and the ratio between tube length and diameter is more than 10. (Incropera et al. 2011, 544.) If there is a large variation of flow characteristics, the correlation of Sieder and Tate can be used.

$$Nu_D = 0{,}027 Re_D^{4/5} Pr^{1/3} \left(\frac{\mu}{\mu_s}\right)^{0,14} \quad (3.8.8)$$

This correlation is valid when the Prandtl number is between 0,7-16 700, Reynolds number is over 10 000 and the ratio between tube length and diameter is over 10. When the Reynolds number has a large variation and the tube surface is smooth, the Gnielinski correlation can be used. It is valid when the Prandtl number is between 0,5-2000 and Reynolds number is between 3000- $5 \cdot 10^6$.

$$Nu_D = \frac{(f/8)(Re_D - 1000)Pr}{1 + 12{,}7(f/8)^{1/2}(Pr^{2/3} - 1)} \quad (3.8.9)$$

4 COMPARISON BETWEEN GAS TURBINE HEAT RECOVERY CALCULATION PROGRAMS

Heat exchangers can be classified based on row arrangement and construction type. There can be heat exchangers with parallel, counter and cross flows. Tubes can be finned or plain. Cross-flowing fluid can be mixed or unmixed. Different construction types of the heat exchangers are concentric tube heat exchangers, cross-flow heat exchangers, shell-and-tube heat exchangers and plate heat exchangers. An important factor in dimensioning heat exchangers is to achieve as large as possible surface are per unit volume. In compact heat exchangers the arrays of finned tubes are used in cases where at least one of the fluids is gas. (Incropera et al. 2011, 706-708.)

There are two typical engineering problems while dimensioning heat exchangers. First problem is heat exchanger design problem, where the inlet and outlet temperatures of the fluid are known in advance. The main problem is specifying the heat transfer surface area and the type of the heat exchanger.

Second problem is heat exchanger performance calculation, where the flow rates and inlet temperatures are known. The problem is to specify the heat transfer rate and fluid outlet temperatures. (Incropera et al. 2011, 730.)

The NTU-method can be used to solve these heat exchanger dimensioning problems. First the effectiveness and heat capacity rates are calculated. After this the NTU value can be determined and then the heat transfer area can be solved. After this the actual heat transfer rate can be defined. (Incropera et al. 2011, 730.)

4.1 Effect of radiation

Radiation between two or more surfaces depends on the geometry, radiative properties and temperatures of surfaces. To establish the impact of the geometrical features, the view factor has to be defined. It can be defined as *"fraction of the radiation leaving surface i that is intercepted by surface j."* There are a couple of relations and rules to ease the calculation of the view factor. (Incropera et al. 2011, 862-863.)

$$A_i F_{ij} = A_j F_{ji} \tag{4.1.1}$$

where	A_i	area of the surface i	[m^2]
	A_j	area of the surface j	[m^2]
	F_{ij}	view factor from i to j	[-]
	F_{ji}	view factor from j to i	[-]

First is reciprocity relation which can be defined with equation (4.1.1).

$$\sum_{j=1}^{N} F_{ij} = 1 \tag{4.1.2}$$

Second rule is summation rule which can be determined with equation (4.1.2). Equations for some geometries have been calculated and they can be used while defining view factors for related geometries. In figure 4.1 the view factor for parallel plates with midlines connected by a perpendicular system can be seen. (Incropera et al. 2011, 865.)

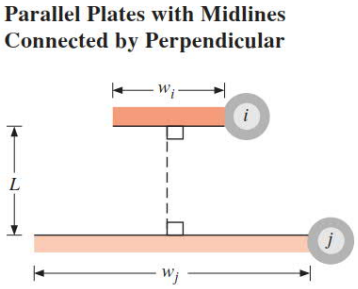

Figure 4.1: View factor for parallel plates with midlines connected with perpendicular (Incropera et al. 2011, 865.)

In figure 4.2 the view factor of the perpendicular plates with a common edge can be seen.

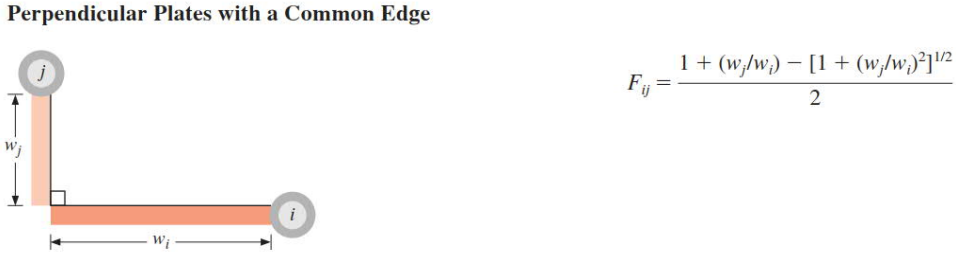

Figure 4.2: View factor for perpendicular plates with a common edge (Incropera et al. 2011, 866.)

In three-dimensional geometries the equations of the view factors can be complicated. Therefore, there are some diagrams for different geometries that can be used to define certain view factor. Factor for aligned parallel rectangles can be defined from figure 4.3.

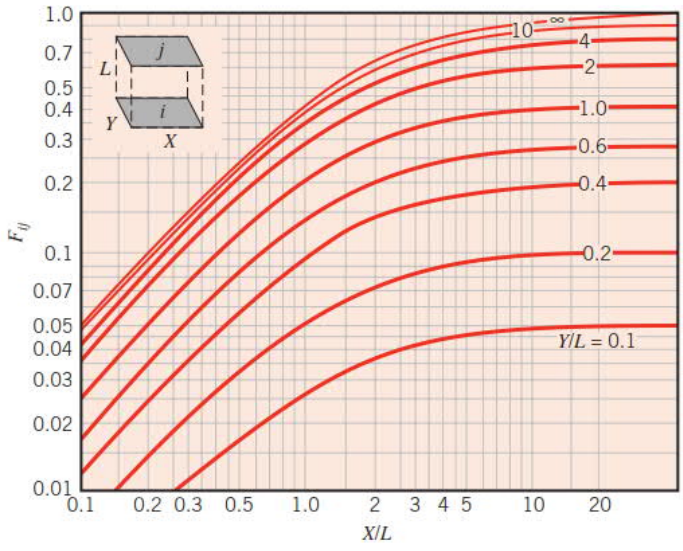

Figure 4.3: View factor for parallel rectangles which are aligned (Incropera et al. 2011, 868.)

For the coaxial parallel disks, the view factor can be determined from figure 4.4.

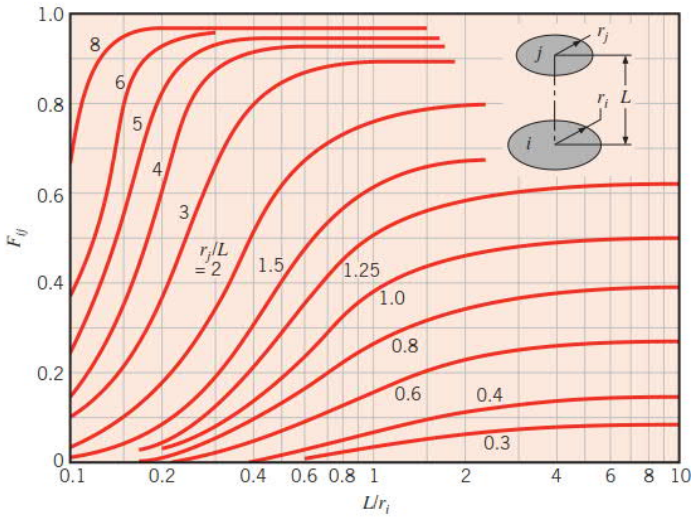

Figure 4.4: View factor of parallel disks which are coaxial (Incropera et al. 2011, 868.)

For the perpendicular rectangles with a common edge, the view factor can be defined with the figure 4.5.

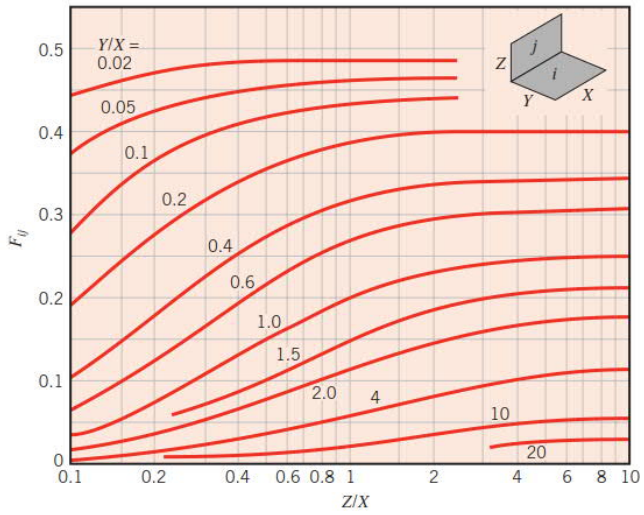

Figure 4.5: View factor of the perpendicular rectangles with a common edge (Incropera et al. 2011, 869.)

4.1.1 Radiation with participating gas media

In this study there is a waste heat recovery boiler and the radiation exchange occurs outside the water tubes in a space with exhaust gases. Exhaust gases consist, for example, of CO_2, H_2O vapor and NO_x which emit and absorb radiation over a wide temperature range. Before in chapter 4.1 the radiation exchange was about surfaces but when it comes to gaseous radiation it depends on volume of the fluid. In spectral radiation, the gas absorption is a function of absorption coefficient κ_λ and medium thickness L.

One tool to define medium absorptivity is Beer's law. To define medium absorptivity, the transmissivity τ_λ has to be calculated. (Incropera et al. 2011, 896-897.)

$$\tau_\lambda = \frac{I_{\lambda,L}}{I_{\lambda,0}} = e^{-\kappa_\lambda L} \tag{4.1.3}$$

where	τ_λ	transmissivity	[-]
	$I_{\lambda,L}$	intensity at the thickness	[-]
	$I_{\lambda,0}$	monochromatic beam of intensity	[-]
	κ_λ	absorption coefficient	[1/m]
	L	thickness of the medium	[m]

Transmissivity can be solved with equation (4.1.3).

$$\alpha_\lambda = 1 - \tau_\lambda = 1 - e^{-\kappa_\lambda L} \tag{4.1.4}$$

where	α_λ	absorptivity	[-]

Absorptivity can be calculated with equation (4.1.4).

If the Kirchhoff's law is valid, the emissivity and absorptivity are equal. Radiant heat flux from the gas to an adjacent surface has to be calculated.

This is called Hottel method where radiation emission is defined from gas temperature to surface element temperature. Emission from the gas can be calculated for a surface area unit as follows. (Incropera et al. 2011, 897.)

$$E_g = \varepsilon_g \sigma T_g^4 \quad (4.1.5)$$

where	E_g	emission from gas	[-]
	ε_g	emissivity of the gas	[-]
	σ	Stefan-Boltzmann constant	[-]
	T_g	temperature of the gas	[K]

Emissivity of the gas in equation 4.1.5 can be correlated with gas temperature, total pressure of the gas and radius of the hemisphere. In exhaust gases water vapor and carbon dioxide are together in a mixture. (Incropera et al. 2011, 897.) Total gas emissivity can be defined as

$$\varepsilon_g = \varepsilon_w + \varepsilon_c - \Delta\varepsilon \quad (4.1.6)$$

where	ε_w	emissivity of the water vapor	[-]
	ε_c	emissivity of the carbon dioxide	[-]
	$\Delta\varepsilon$	correction factor of emissivity	[-]

Emissivity of the water vapor can be defined from figure 4.6 when the total pressure is 1-atm.

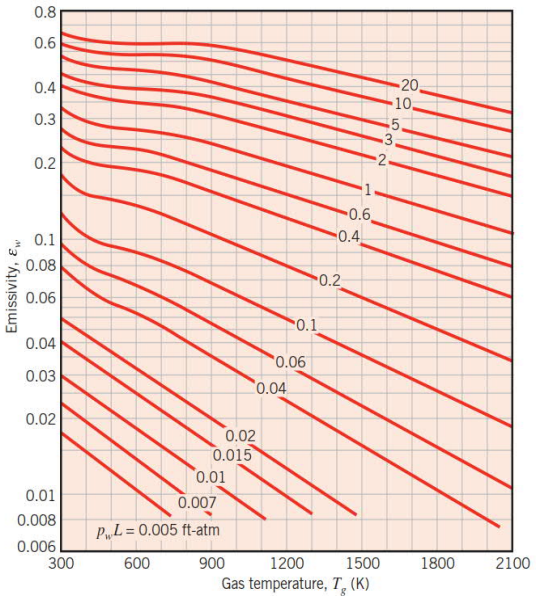

Figure 4.6: Emissivity of the water vapor when the total pressure is 1-atm (Incropera et al. 2011, 898.)

Emissivity of the carbon dioxide in a mixture of the gases can be defined from figure 4.7 when the total pressure is 1-atm.

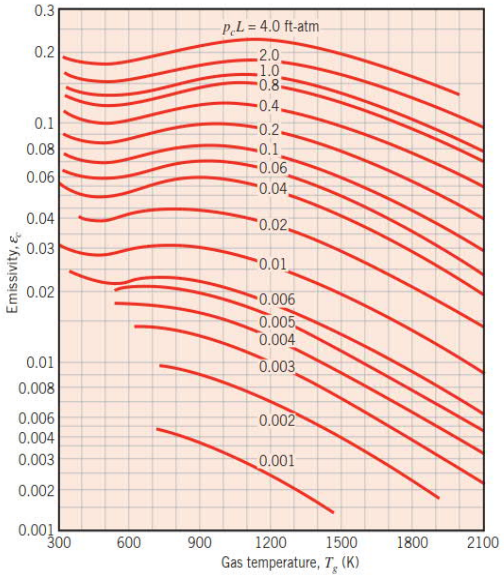

Figure 4.7: Emissivity of the carbon dioxide when the total pressure is 1-atm (Incropera et al. 2011, 899.)

Pressure correction factor C_c for carbon dioxide can be determined from figure 13.19 when the total pressure is other than 1-atm. Correction factor $\Delta\varepsilon$ for the mixture of water vapor and carbon dioxide can be examined in the figure 4.8. (Incropera et al. 2011, 900.)

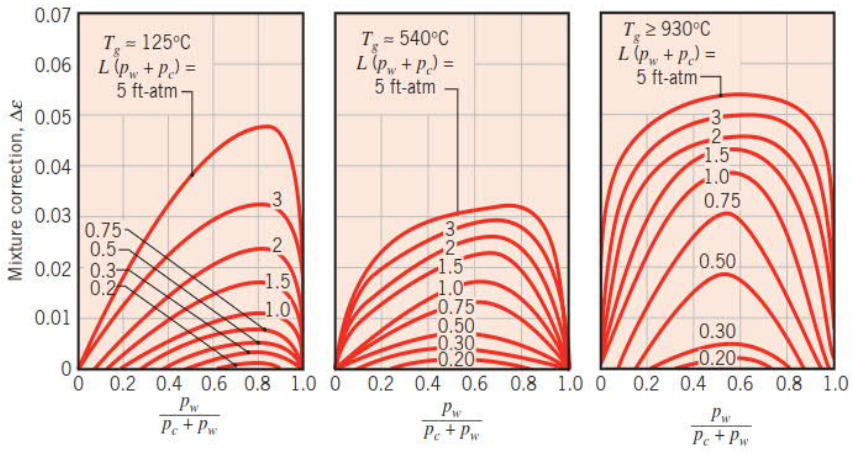

Figure 4.8: Correction factor for the mixture of the water and carbon dioxide (Incropera et al. 2011, 900.)

Radiant heat transfer rate to the surface can be solved with

$$q = \varepsilon_g A_s \sigma T_g^4 \tag{4.1.7}$$

For other gas geometries than a hemispherical gas mass the mean beam length L_e is used instead of thickness of the medium. (Incropera et al. 2011, 900). Mean beam length can be defined from table 4.1.

Table 4.1: Mean beam lengths for different gas geometries (Incropera et al. 2011, 900.)

Geometry	***Characteristic Length***	L_e
Sphere (radiation to surface)	Diameter (D)	0,65D
Infinite circular cylinder (radiation to curved surface)	Diameter (D)	0,95D
Semi-infinite circular cylinder (radiation to base)	Diameter (D)	0,65D
Circular cylinder of equal high and diameter (radiation to entire surface)	Diameter (D)	0,60D
Infinite parallel planes (radiation to planes)	Spacing between planes (L)	1,80L
Cube (radiation to any surface)	Side (L)	0,66L
Arbitrary shape of volume V (radiation to surface of area A)	Volume to area ratio (V/A)	3,6V/A

Radiant heat transfer rate that is calculated with equation 4.1.7 shows the rate in the mean gas temperature. Net heat transfer rate is defined between temperatures of gas and surface. (Incropera et al. 2011, 901.)

$$q_{\text{net}} = A_s\sigma\left(\varepsilon_g T_g^4 - \alpha_g T_s^4\right) \tag{4.1.8}$$

where q_{net} net rate of heat transfer [W]

α_{g} absorptivity of the gas [-]

T_{s} temperature of the surface [K]

Absorptivity of the gas mixture which is a part of equation (4.1.8) can be calculated with separate absorptivities of water vapor and carbon dioxide.

$$\alpha_w = C_w\left(\frac{T_g}{T_s}\right)^{0,45} \cdot \varepsilon_w\left(T_s, p_w L_e \frac{T_s}{T_g}\right) \tag{4.1.9}$$

where α_{w} absorptivity of the water vapor [-]

C_{w} pressure correction of water vapor [-]

	p_w	pressure of water vapor	[Pa]
	L_e	mean beam length	[m]

Absorptivity of the water vapor can be calculated with equation (4.1.9). Mean beam length and pressure correction factor are used to solve the value of the absorptivity.

$$\alpha_c = C_c \left(\frac{T_g}{T_s}\right)^{0,65} \cdot \varepsilon_c \left(T_s, p_c L_e \frac{T_s}{T_g}\right) \quad (4.1.10)$$

where	α_c	absorptivity of the carbon dioxide	[-]
	p_c	pressure of the carbon dioxide	[Pa]

Absorptivity of the carbon dioxide can be calculated with equation (4.1.10).

$$\alpha_g = \alpha_w + \alpha_c - \Delta\alpha \quad (4.1.11)$$

where	$\Delta\alpha$	correction factor of absorption	[-]

Absorptivity of the gas mixture can be calculated with equation (4.1.11) and after that it can be inserted to equation (4.1.8) to solve the net heat rate.

4.2 GE2-Select

GE2-Select is one of the calculation programs used by Alfa Laval Aalborg Oy for gas turbine waste heat recovery solutions. It has been in use in the late 90's and in early 2000s. GE2-Select is an excel based dimensioning program for solid finned tubes. There are various sheets for input data, output data, and substance properties for exhaust gases and water. In this calculation program, dimensioning is done for both staggered and aligned tube arrangements. Radiation heat transfer has not been considered. (Läiskä 2001.) Equations of this calculation program are presented in Appendix 1.

4.2.1 Input values and start of the calculation

There is some input data for scope of supply. The number of boilers can be chosen as well as whether or not there is a bypass duct, insulation or instrumentation. Maximum exhaust gas (EG) temperature is also a part of scope of supply input data. There are also input data for tubes: Fin pitch – the number of fins per meter can be chosen. Also, the spiral fin tube length and number of tubes across can be given. The number of header nozzles and exhaust gas flange size are input data. There are also system input data for both exhaust gas and water. For exhaust gas the given values are mass flow rate, inlet temperature and outlet temperature. For water the given input values are inlet and outlet temperatures. Air factor of the boiler is also an input value.

Dimensioning begins with choosing the flow arrangement of the boiler and both radiation and bypass losses. The flow arrangement can be parallel or counter flow. Specific heat capacity of the exhaust gases comes from the gas properties sheet when the inlet and outlet temperatures of the exhaust gas are known. With the specific heat capacity and temperatures, the inlet and outlet enthalpies can be calculated. The density of the exhaust gas comes from the gas properties sheet too. Total thermal power of the boiler can be calculated with specific heat capacity, mass flow rate of the exhaust gases and temperature difference between inlet and outlet exhaust gas temperatures. The volumetric flow rate of the exhaust gas is defined when the mass flow rate and density are known.

When the inlet and outlet temperatures of the water are known, the density, specific heat capacity and inlet and outlet enthalpies can be obtained from the water properties sheet. When the total thermal power of the boiler is known the mass flow rate of the water is calculated. After the mass flow rate of water is known, the volumetric flow rate of the water is solved. Average temperature of the water is calculated as well as the log mean temperature. Log mean temperature difference is calculated for the chosen flow arrangement. After the log mean temperature has been calculated and the thermal power of the boiler is known, the required conductance is defined.

4.2.2 Heat transfer surfaces

Some dimensions for tubes, such as the outer diameter and wall thickness which in turn define the inner diameter, and for fins such as fin distribution and average thickness can be chosen. Also, the height of the fin can be chosen and tube distribution in the direction of and against the direction of the flow are selected. The number of inlets can be calculated as well as the outer diameter of the fin.

When these dimensions are selected and calculated the *fin area for a tube* can be solved. Furthermore, the *area between the fins for a tube* is calculated. After these two areas are defined, the *effective total heating surface* can be solved. The surface area ratio for fins and for tube can be determined when the fin area, area between fins and total heating surface are all known.

4.2.3 Internal heat transfer

Internal heat transfer happens on the water side. The density and specific heat capacity of water have been picked earlier from the water properties sheet. Now thermal conductivity, and kinematic and dynamic viscosities can be obtained from the water properties sheet. The total inner area of the tubes can be calculated when the inner diameter and the number of the tubes are known.

The velocity of the water flow can be solved when the inner area of the tubes has been calculated and the volumetric flow of the water has been defined earlier. Now the Reynolds number can be calculated with the known flow velocity. Also, Prandtl number for the internal flow of the tube is calculated. After Reynolds and Prandtl numbers have been solved, the convective heat transfer coefficient can be defined.

4.2.4 External heat transfer

External heat transfer calculations are done for the exhaust gas flow side. Average temperature of the exhaust gas is calculated. Density, specific heat capacity for exhaust gas,

thermal conductivity as well as kinematic and dynamic viscosities can all be picked from the gas properties sheet.

Heat transfer for tubes is determined first. Area of the free cross-section can be calculated separately for staggered and aligned tube arrangements. When the area of the free cross-section is solved, the velocity of the exhaust gas can be determined, which in turn can be used to calculate the Reynolds number. After that the Prandtl number is defined. Direction factor, that is defined separately for staggered and aligned tube arrangements, can be calculated when the Reynolds number is solved. With Prandtl and Reynolds numbers the Nusselt number for the external flow can be solved. Convection heat transfer coefficient for tubes in external flow can be calculated after the Nusselt number is known.

Next the heat transfer for the fins is defined. The total length of the fin is calculated and then the thermal conductivity of the fin material in the mean temperature is chosen. After that the convection heat transfer coefficient for the fins in the external flow can be solved.

4.2.5 Total heat transfer

First the external total heat transfer is calculated by solving the total value of the convection heat transfer coefficient, that consists of the fin coefficient and the gas side coefficient. These values are also multiplied with surface area ratios for the fins and tube surfaces. Thermal conductivity of the tube material in the mean temperature is picked and it can be fed to the calculation program. The total heat transfer surface for inside of the tube is calculated for a single tube. After that the logarithmic total heat transfer surface area can be solved. Thickness of the tube wall is defined enabling the calculation of a theoretical k-value. A clean k-value can be calculated when the k-value fouling factor is chosen. A dirtiness factor is chosen and after that the real k-value can be calculated.

4.2.6 Pressure loss of the external and internal flow of the tubes

The direction factor for the pressure is calculated separately for staggered and aligned tube arrangements and it can be solved for this pressure if the outer diameter and tube distribution against the flow are known.

Hydraulic length of the fin is defined with heights and distribution of the fins. The cross-sectional area free flow is calculated and after that the hydraulic diameter can be determined. The length of the fin can be defined when the outer diameter of the tube and height of the fin are known. After the length of the fin is defined, the pressure loss for the external gas flow can be calculated. The pressure loss inside the tube can be calculated when the effective tube length, internal tube diameter and the velocity of the water flow are all known.

4.2.7 Dimensioning

The dimensioning begins with defining the requirement of the heat transfer surface area. This can be calculated when the required conductance and the clean k-value are known. Next step is to determine the heat transfer surface per a row. It is done by dividing the effective total heat transfer surface for one row with number of tubes across. The theoretical number of tube rows is calculated with the need of the heat transfer surface area and heat transfer surface per a row. Total number of tube rows can be defined by rounding the theoretical number of tube rows up.

After the number of tube rows has been defined, the number of tubes can be solved. The rounding marginal is calculated as well as the total heat transfer surface. The number of times the water tube passes over the gas channel is determined. Also, the overall marginal is defined. Finally, the entire pressure loss of the gas and water flows are calculated.

4.3 EGB GS 1999

EGB GS 1999 is one of Alfa Laval Aalborg's calculation programs for gas turbine waste heat recovery solutions. It has been in use in the late 90's. EGB GS 1999 is an excel based dimensioning program for solid finned tubes. There is a sheet for water properties. In this calculation program, dimensioning is done for a staggered arrangement. (Alfa Laval Aalborg 1999.) Equations of this calculation program are presented in Appendix 2.

4.3.1 Input data and preparation for dimensioning

Dimensioning of the boiler or boilers starts by choosing some input data. First the numbers of boilers, circulation water pumps per a boiler and steam drums are chosen and fed to the dimensioning program. In this program it can be chosen if the superheater, economizer, by-pass or condenser is wanted to be part of the scope of supply. The exhaust gas flow from the engines is one of the input values and it can be fed to the program. Basic properties of the exhaust gases are often known and in this program the inlet and outlet temperatures of the exhaust gas are known. Maximum pressure drop of the exhaust gases can be defined for input values. The feed water temperature and the pressure of the live steam are given for input values and dimensioning. A preset fouling margin can also be defined. An approach temperature of the exhaust gas can be given but it is not necessary to give it.

Calculations in preparation of dimensioning begin with calculating the specific heat for exhaust gas in an average temperature using an experimental correlation. Density of the exhaust gas is defined next with another correlation. When the density is defined and the mass flow rate of the exhaust is known, the volumetric flow rate can be calculated by dividing the mass flow rate with the density. The caloric losses are chosen, and the total output of the exhaust gases can be calculated.

Temperature of the saturated steam is defined on the separate water properties sheet. When the steam pressure, and the superheating, approach, and feed water temperatures are known the enthalpy of the superheated steam can be calculated with an experimental equation. Next the enthalpy of the saturated steam is determined and also the approach enthalpy is calculated, and again calculations are made with an experimental equation. After this the enthalpy of the feed water can be defined.

Next the outputs of the superheater, evaporator and economizer are calculated. If there is a superheater in the system, its output is calculated. The output power is zero if there is no superheater. If there is an economizer in the system, the output power of economizer is defined, and the output power of the evaporator is calculated with enthalpy of the saturated steam and enthalpy in temperature of approach. If there is no economizer, the output power is zero and the output power of evaporator is calculated with enthalpy of saturated steam and

feed water. The total output power of the whole system is calculated by adding all partial output powers together.

Approximate mean temperatures in the superheater, evaporator and economizer are solved as well as the corresponding specific heats. First the calculation is made for the superheater if it is part of the system. Also, the specific heat calculation in the mean temperature is done. The same procedure is done also for the evaporator and economizer. Specific heats are defined with experimental equations. The temperature of the exhaust gas decreases while it flows through the boiler system and this can be calculated separately in different boiler sections.

Mean temperatures between the exhaust gas inlet temperature and temperature after superheater, temperatures after superheater and evaporator, and temperatures after evaporator and economizer are calculated. Temperature after the evaporator can be chosen. After this the logarithmic temperatures and conductances for superheater, evaporator and economizer are defined. The exhaust gas density in different sections is solved and permissible pressure drop in the evaporator is defined. After that the pipe length is determined. Pipe length can be given manually or calculated in the program according the flow.

4.3.2 Evaporator

In the dimensioning program there is table for the evaporator where as a function of rows in high, some values are listed; for example, rows in width, gas velocity, k-value and conductance. First the gas velocity is calculated for all the rows in height values. Also, the exhaust gas density at and the maximum pressure drop in the evaporator. Calculation is made with an experimental equation. After that the number of rows in width is defined when the velocity of exhaust gas and length of the pipe are known parameters. The k-value can be calculated with an experimental equation. After that the available conductance is calculated for all rows in height and is compared with command “Index” to the previously calculated required conductance. When the comparison is done the actual number of rows in height and width are known, as well as are the actual gas velocity and k-value. With the required and

available conductances, the margin for this calculation can be solved. After this the pressure drop in the evaporator is calculated and heating surface area is defined for the evaporator.

4.3.3 Superheater

When the dimensions for the evaporator are defined, calculations can advance to the superheater. In the dimensioning program there is also a table for the superheater where as a function of rows in height, some values like the gas velocity, k-value and conductance are listed. Number of rows in width is always the same that it is in the evaporator.

First the gas velocity is calculated for all the rows in height values. Also, the density at and the pressure drop in the superheater must be known. Calculation is made with an experimental equation. K-value is calculated with an experimental equation. After that the available conductance is calculated for all rows in height and is compared with command “Index” to the previously calculated required conductance. When the comparison is done the actual number of rows in height and width are known as well as the actual gas velocity and k-value. With the required and available conductances, the margin for this calculation can be solved. After this the pressure drop in the superheater is calculated and heating surface area is defined for superheater.

4.3.4 Economizer

When the dimensions for the superheater are defined, calculations can be furthered to the economizer. In the dimensioning program there is also table for the economizer where as a function of rows in high, some values are listed for example gas velocity, k-value and conductance. Number of rows in width is always the same that it is in the evaporator.

First the gas velocity is calculated for all the “rows in height” values. Also, the density at and the pressure drop in the economizer must be known. Calculation is made with an experimental equation. The k-value is calculated with an experimental equation. After that the available conductance is calculated for all rows in height and is compared with command “Index” to previously calculated required conductance. When the comparison is done the actual number of rows in height and width are known as well as the actual gas velocity and

k-value. With the required and available conductances, the margin for this calculation can be solved. After this the pressure drop in the economizer is calculated and heating surface area is defined for economizer.

4.3.5 Final calculations

If there is a superheater in a system, the mass flow rate for the steam can be calculated with the enthalpy in the superheater. If there is no superheater, the used enthalpy is the enthalpy of saturated steam. The total heating surface can be calculated when the number of rows in height and in width are known and the length of one pipe is calculated. All of these are multiplied together, and the result is multiplied with a factor which can be chosen. Also, the total pressure drop for whole system is calculated by adding the different components together. The total size of the boiler can be defined when the dimensions of the pipe bundle are known. In the final calculations the dimensions of the auxiliaries are solved. First the capacities, pressures, and electrical motor requirements of circulation pumps are defined. Also, the same values for feed water pumps and the feed water tank are calculated and defined.

4.4 Comparison between GE2-Select and EGB GS 1999

In this chapter the differences and similarities of different dimensioning programs are analyzed. Correctness' of calculations are examined, and processes of dimensioning compared. Dimensioning of the boilers begin with deciding the number of boilers. In GE2-Select the scope of supply is defined with the existence of the bypass duct, insulation and instrumentation. For EGB GS 1999 values that define the scope of supply are the number of circulation pumps per boiler and steam drums. Furthermore, the existence of superheaters, economizers and by-passes are determined. Only in GE2-Select the dimensions and parameters of water tubes are given. Fin pitch of the tubes, spiral fin tube length and number of tubes across are defined. Also, the number of header nozzles and exhaust gas flange size is a part of input data. System input data parameters are quite similar in both dimensioning programs; Exhaust gas mass flow rate is given as well as inlet and outlet temperatures of exhaust gas. In GE2-Select inlet and outlet temperatures for the water side are defined, but

in EGB GS 1999 only the feed water temperature and pressure of the steam are given. The maximum pressure drop for the exhaust gases, fouling margin and approach temperature of the exhaust gases are given only in EGB GS 1999. Air factor is input value only in GE2-Select.

In GE2-Select the flow arrangement can be chosen to be parallel or counterflow, while in EGB GS 1999 calculation only works for counterflow. In both programs caloric losses are defined. In GE2-Select they can be given to the program, but in EGB GS 1999 value of losses can be chosen from two values based on the existence of a by-pass duct. The main difference between these two programs is the origin of properties of water and exhaust gas. In GE2-Select there are separate properties sheets for water and for exhaust gas, while in EGB GS 1999 all the properties have been calculated with experimental equations.

Solving the specific heat of the exhaust gases and the result using the result to obtain the necessary data from gas properties sheet or solving it with experimental equation gives almost the same result. Density of the exhaust gas with the same input values is different between direct calculations and getting data from the gas properties sheet. It can be assumed that the program with a properties sheet is more trustworthy than the one with experimental equations. If all the equations make small deviations to the tabled values, in the end the total difference can grow to be quite a big one. On the water side these differences can be assumed to be small, but large differences can occur on the exhaust gas side. Results of the calculations can have major differences because of the properties and assumptions made for exhaust gas in these dimensioning programs.

Next the calculations continue quite similarly in both programs. The next difference is that the log mean temperature difference for the whole system is calculated only in GE2-Select. This dimensioning program is based on LMTD-method. Reynolds, Nusselt and Prandtl numbers are solved to get the right output. EGB GS 1999 does not fully use neither the LMTD- or NTU-method in the dimensioning. These are the basic heat exchanger dimensioning tools and a waste heat recovery boiler is basically a big heat exchanger. In EGB GS 1999 the log mean temperature difference is calculated separately for the superheater, evaporator and economizer. This is used to solve the required conductance for

each component of the system. The dimensioning in EGB GS 1999 is based on comparing the required and available conductances for each component and getting the amount of tubes from there.

Correlations used in GE2-Select are not directly the widely known correlations like Zukauskas. They are mildly modified, but the original ones can be recognized. Partly experimental equations can be assumed to work better than fully experimental ones. Margin of error can also be assumed to be smaller in GE2-Select than EGB GS 1999. Dimensions of the tubes are given only as input values for GE2-Select. The tube diameter, length and wall thickness are given for this dimension program. In EGB GS 1999 the tubes are assumed to be standard sized. In both dimensioning tools, correction factors are used. They are a part of the correlations and are different in both tools. In GE-2 design the direction factor, fouling factor and direction factor for pressure are defined separately, but in EGB GS 1999 these are part of the correlations except for the fouling factor.

4.5 Calculation comparison between programs

In this chapter the calculation example with imagined values is presented and the results are compared. Differences between the size of heat transfer surfaces, number of tubes and exhaust gas side pressure loss, are analyzed. The input values for this calculation example are given in table 4.2. Calculation is made with nine different cases. Only changing parameters are the exhaust gas mass flow rate and inlet temperature. Other parameters remain constant for all the cases.

Table 4.2: Input values for calculation example

	EG mass flow rate [kg/s]	EG inlet temp [°C]	EG outlet temp [°C]	Feed water temp [°C]	Superheating temp [°C]	Approach temp [°C]
Case 1	25	500	200	95	300	20
Case 2	30	500	200	95	300	20
Case 3	35	500	200	95	300	20
Case 4	25	550	200	95	300	20
Case 5	30	550	200	95	300	20
Case 6	35	550	200	95	300	20
Case 7	25	600	200	95	300	20
Case 8	30	600	200	95	300	20
Case 9	35	600	200	95	300	20

Calculations are made with the typical contents of the exhaust gas which is used in dimensioning usually for gas turbine solutions. Calculation is made with GE-2 Select and EGB GS 1999. Other calculation programs that have been used in Alfa Laval Aalborg Oy in 1990s and early 2000s are dos-based WHR Boiler Select and application-based ABC-design. Because ABC-design is made originally for customer and therefore it gives only total power output as result. In both calculation programs the impact of the radiation from the exhaust gas to the fins is assumed to be negligible. Parameters that can be gotten as a result from sales tools cannot be obtained from ABC-design program, and therefore it is not reviewed in this thesis. The dos-based WHR Boiler Select is difficult to use, old fashioned, and not very user friendly. In this program the user defines the number of tubes and the heat transfer area. The only parameter generated by the program and could be analyzed in this thesis is pressure loss of the exhaust gas. Because of these reasons this dimensioning tool is not reviewed in this thesis.

First the heat transfer surface is calculated for nine different cases with GE2-Select and EGB GS 1999. Results of the calculations are presented in figure 4.9.

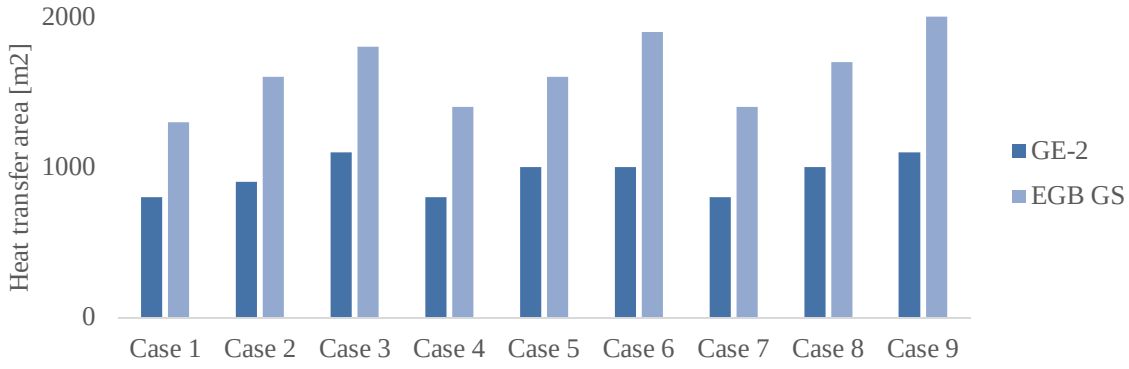

Figure 4.9: Heat transfer area calculated with GE2-Select and EGB GS 1999 programs and with nine different cases

Differences between two programs are quite large in regard to the heat transfer area. Because almost only experimental equations are used in EGD GS 1999, it can be assumed that the difference comes from the experimental factors. Also, the properties of the exhaust gases have been solved from experimental correlations in EGB GS 1999 and it can cause some errors in calculation. In GE2-Select properties of water/steam and exhaust gas are coming from table of values that can be assumed to be accurate. Also, correlation used are known from the literature.

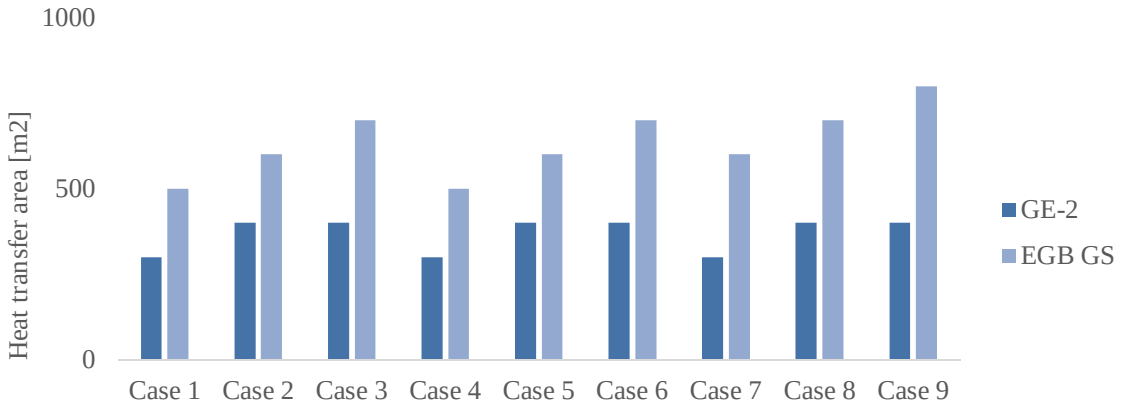

Figure 4.10: Number of tubes calculated with GE2-Select and EGB GS 1999 with nine different cases

Next the number of tubes is solved for nine cases with GE2-Select and EGB GS 1999. Also, these results vary quite a lot in comparison with each other. Results can be seen in figure 4.10. Difference can be assumed to be caused from the same reasons as the differences with heat transfer surfaces.

The third solved parameter is the exhaust gas pressure drop. This is also calculated for nine cases with GE2-Select and EGB GS 1999. Results can be seen from figure 4.11.

Figure 4.11: Exhaust gas pressure drop calculated with GE2-Select and EGB GS 1999 with nine different cases

It can be noticed that GE2-Select takes variations in mass flow rate of the exhaust gas into account while calculating the pressure drop. EGB GS 1999 does not do that and the pressure drop is quite constant for all nine cases. It can be assumed that mass flow rate should affect to value of the pressure drop. All in all, GE2-Select gives more accurate and sensible results than EGB GS 1999. Calculation methods in these two programs are different and EGB GS 1999 uses much more experimental equations and factors.

5 UPDATE TO SALES TOOL

In this chapter the dimensioning and sales program owned by Alfa Laval Aalborg Oy is presented generally and its integration to the whole system is described. Furthermore, the new created update block for sales tool is presented as well as the T-Q -diagrams generated with it.

5.1 Sales tool in general

The sales tool includes many different sales and dimensioning tools in addition to boiler dimensioning and budget calculations. Other main functions of the sales tool are the creation of technical specifications, and transferring information to ERP-tools, which are other programs used by Alfa Laval Aalborg Oy. (Alfa Laval Aalborg Oy, 2018.). The sales tool is also connected to the document and project management systems.

5.2 GT WHR calculation update

Different technical solutions can be designed with iPro, but at the moment the specific dimensioning tool for gas turbine waste heat recovery boilers is missing. The Gas Turbine Waste Heat Recovery (GT WHR) tool consists of 10 different parts of calculation. First two are primary input data and finned tube input data where the inlet and outlet temperatures of the exhaust gas are given, as well as finned tube dimensions and other input parameters. Because both inlet and outlet temperatures are known the calculation in this tool is made with LMTD-method. Next part is the scope of supply. Exhaust gas input data and exhaust gas content calculation are the next parts of the calculation tool. Density and specific heat value are solved in the exhaust gas content part.

The heat surface of a single finned tube is solved next with spiral serrated fin solution. Water side heat transfer calculations are made separately for the superheater, economizer and evaporator. Convective heat transfer coefficient is solved for each heat transfer equipment. On the exhaust gas side, the calculations are made for aligned and staggered tube arrangements. Calculations are also solved separately for the superheater, evaporator and economizer. After that the heat transfer in the fins is determined for the superheater,

evaporator and economizer. The total heat transfer in the system can be calculated when the heat transfer in both inside and outside of the tubes is determined and the heat transfer in the fins is solved. K-values are solved and can now be used in calculating the number of tubes and total heat transfer surface. These are separately solved for the evaporator, superheater and economizer. Results are collected to total output part where the total output power, feed water flow, pinch points for each heat transfer surface, number of tubes and total pressure drop are presented.

Table 5.1: Initial values for example calculations with gas turbine WHR dimensioning tool

	EG mass flow rate [kg/s]	EG inlet temp [°C]	EG outlet temp [°C]	Feed water temp [°C]	Superheating temp [°C]	Approach temp [°C]
Case 1	30	500	200	95	300	20
Case 2	35	500	200	95	300	20
Case 3	30	550	200	95	300	20
Case 4	35	550	200	95	300	20
Case 5	30	600	200	95	300	20
Case 6	35	600	200	95	300	20

Calculations are made with constant fin dimension values. Only the exhaust gas mass flow rate and inlet temperature are changing in different cases. Mass flow rate differs between 30-35 kg/s and inlet temperature differs between 500-600 °C.

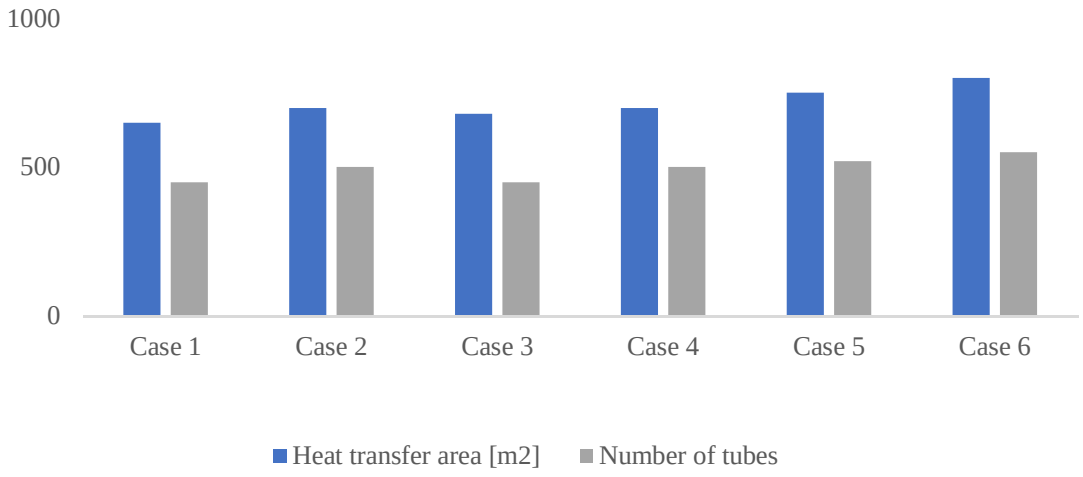

Figure 5.1: Heat transfer area and number of tubes calculated with 6 different cases

From figure 5.1 can be seen that when the exhaust gas mass flow rate and inlet temperature are increasing also the number of tubes and heat transfer area are getting bigger. When the exhaust gas inlet temperature is 500 – 550 °C, the results are quite constant. After the inlet temperature reaches 600 °C the number of tubes and heat transfer surface are increasing.

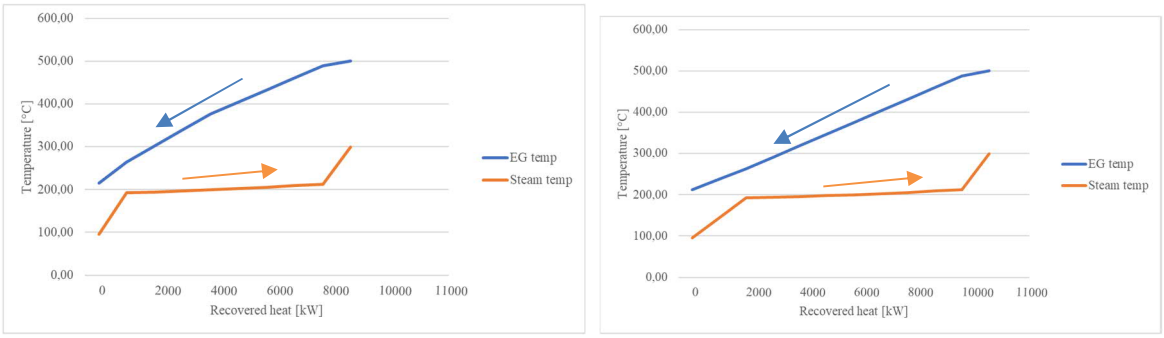

Figure 5.2: T-Q -diagrams with Case 1 (left) and Case 2 (right) input values. Arrows indicate the direction of the temperature change in the process.

In cases 1 and 2 the exhaust gas inlet temperature is 500 °C. Therefore, the blue line (exhaust gas) starts and ends to the same point in both diagrams. In case 1 the mass flow rate of exhaust gas is 30 g/s and for case 2 it is 35 kg/s. It can be noticed that the change in mass flow rate affects the total power output of the system. The bigger the mass flow rate is the bigger also the total output is. The difference between the outputs is showing also in shape of the blue curve.

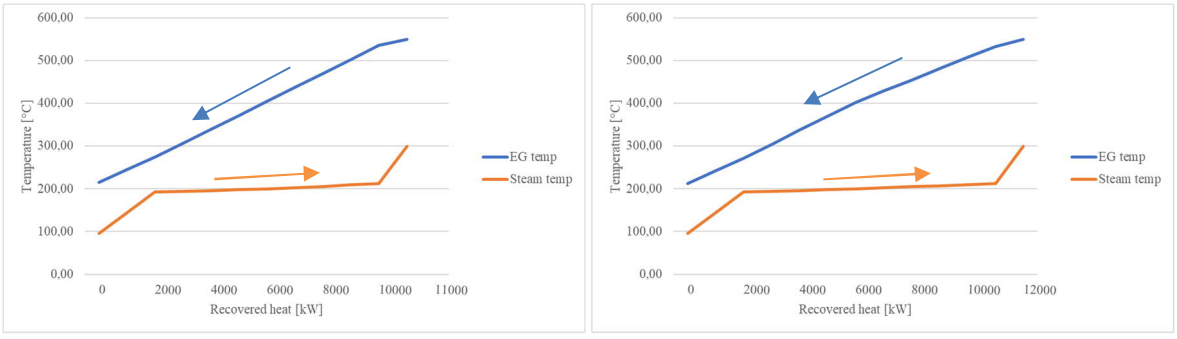

Figure 5.3: T-Q -diagram with Case 3 (left) and Case 4 (right) input values. Arrows indicate the direction of the temperature change in the process.

In cases 3 and 4 the exhaust gas inlet temperature is 550 °C. The total output in case 3 is higher than in previous cases, because the temperature difference between the inlet and outlet temperatures is bigger. Because the feed water and superheating temperatures are constant in all cases, the orange line (steam) starts from the same temperature point and ends also in the same point.

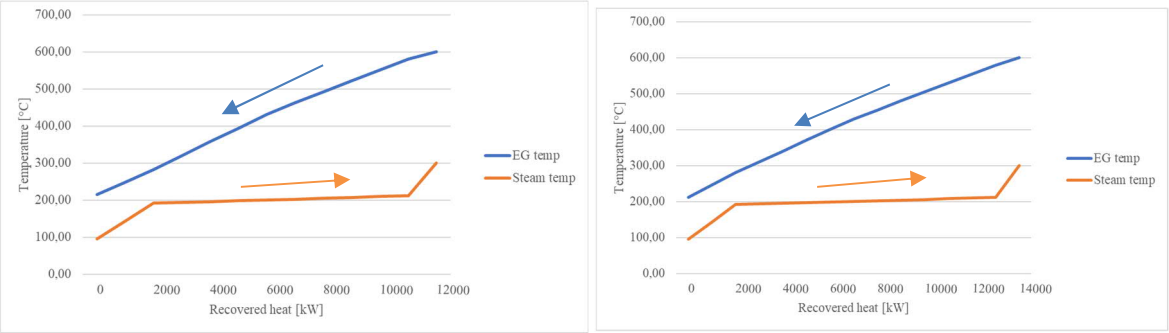

Figure 5.4: T-Q -diagram with Case 5 (left) and Case 6 (right) input values. Arrows indicate the direction of the temperature change in the process.

In cases 5 and 6 the exhaust gas inlet temperature is 600 °C. Both inlet temperature and mass flow rate have an impact to the total output. Because feed water and superheating temperatures are constant in all cases, the orange line (steam) starts from the same temperature point and ends also in the same point also in these two cases.

With Cases 1-6 the impact of radiation heat transfer differs from 0,008-0,015 % when it is compared to the total power output. It can be assumed to be negligible and it has not to be taken into an account in dimensioning.

6 CONCLUSIONS

The Brayton process is usually used in power generation and aircraft propulsion. Power generation can be used as part load units because the startup time of the gas turbine is short. Startups are done usually daily or weekly. Quite often gas turbines are used as top cycles in combined cycles. In the corresponding bottoming cycles, the circulating substance is often water/steam, air or an organic fluid. The bottoming cycle utilizes the waste heat of the gas turbine system, improving the efficiency and power output of the gas turbine. In a normal gas turbine process alone, the efficiency depends on combustion chamber temperature and pressure ratio of the turbine.

The bottoming cycle can also be called Heat Recovery Steam Generator which converts thermal power from the exhaust gas to steam. If there is steam turbine and generator after the system, power can be converted to electricity. This kind of HRSG process has typically more than one pressure levels.

Therefore, there are multiple inlets to the steam turbine and the steam flow in the turbine increases from the inlet to outlet. If there is no additional firing in the HRSG, it is basically a convective heat exchanger. Boilers can be vertical or horizontal. In the past vertical boiler was called a forced circulation boiler and horizontal a natural circulation boiler. There can be sulfur in the natural gas which is used as a fuel of the system. When the sulfur is in the exhaust gases, it can cause corrosion in the cold end of the HRSG -boiler. It is a major designing issue that has to be taken under consideration. Heat transfer surfaces that are in contact with exhaust gases must be in a temperature which is above the sulfuric acid dew point. Designing the boiler is optimization between costs and size of heat transfer surfaces.

There are some special types of gas turbine combined cycles. One of them is Maisotsenko gas turbine cycle (MGTC) which is an air turbine cycle for humid air. The air saturator is used to humidify air for bottoming cycle. Waste heat from the gas turbine is used to heat and humidify the air. When the air is humidified, its heat capacity and mass is increasing. The second waste heat recovery application is called a low temperature economizer, that is used to cool exhaust gases and transfer heat to feed water. In this solution finned tubes are usually

used. The biggest risk in using low temperature economizers is the quickly progressing low temperature acid corrosion. The third special solution is Organic Rankine Cycle (ORC).

In HRSG system the heat transfers mainly via convection. Fins are on the exhaust gas side of the tube, because the convection is more efficient on the water side. In this thesis the convection of the plane wall, finned tubes and overall surface efficiency are described, analyzed and examined. Fins can be considered as extended surfaces of the tubes. Extended surfaces increase the effective surface of the heat transfer. NTU-method and LMTD-methods that are used to design heat exchanger are examined in this master's thesis. Equations for convection, conduction and NTU- and LMTD-method were examined in the chapter 3. External flow of tube banks and internal flow were presented and equations to occur the calculations were examined.

Tubes can be assumed to be cylinders in a cross flow. Behind the row of the tubes, the boundary layer separation occurs when the fluid lacks enough momentum to overcome the pressure gradient. Reynolds number is the most relevant factor to examine the occurrence of the boundary layer transition. When the inlet temperature of the fluid is known and outlet temperatures are specified, the LMTD-method is used. Overall heat transfer coefficient and total surface area can be determined when the LMTD-method is used. Calculations can be made based on energy balances. If only the inlet temperature of the fluid is known, the effectiveness-NTU -method should be used as an alternative solution.

When it comes to consideration of the external flow it has to be known whether the flow is laminar or turbulent. The same should be considered with internal tube flow. Flow should be fully developed. If the flow is laminar, the fully developed velocity profile is parabolic. For a turbulent flow, the velocity profile is flatter.

Heat exchangers can be classified according to row arrangement and construction type. The heat recovery boilers considered in this thesis were cross- and counterflow heat exchangers. Tubes were segmented spiral fins. An important factor in dimensioning heat exchangers is to achieve as large as possible surface (area) per unit volume. There are two typical dimensioning problems when heat exchangers are designed. First is the design problem where the fluid inlet and outlet temperatures are known preliminarily. Problem is to specify

the heat exchanger type and heat transfer surface area. Second problem is about performance calculation. In this problem the flow rates and inlet temperatures are known, but the problem is to specify the heat transfer rate and fluid outlet temperatures.

In this thesis the radiation exchange occurred outside the water tubes in the exhaust gas side in the waste heat recovery boiler. Exhaust gases consist for example of carbon dioxide, water steam and nitrogen oxides which emit and absorb radiation over a wide temperature range. Radiation exchange can be seen as an effect between surfaces or as a volumetric phenomenon. When it comes to gaseous fluids radiation it is about volumetric phenomenon. In the practical part of this thesis the effect of radiation was assumed to be negligible.

Calculation methods with equations were presented for two dimensioning programs which are property of Alfa Laval Aalborg Oy. First of these was GE2-Select which is made for gas turbine waste heat recovery system dimensioning. The program is Excel based and used for solid finned tubes. Calculation was made for both staggered and aligned tube arrangements. The second program that was presented carefully in this thesis was EGB GS 1999. This program was for solid spiral fins with a staggered tube arrangement. The program is also Excel based.

Four dimensioning programs were compared and analyzed with an experimental calculation example. ABC-design and WHR-boiler Select were too old fashioned and hard to use, so they were left out from the comparison. Also, some compared parameters had to be given to these programs as input values, so they did not suit this calculation comparison. Calculation comparison with EGB GS 1999 and GE2-Select was done with nine cases. Results differed a lot and the differences were caused by different calculation methods and experimental equations and factors used in EGB GS 1999. The pressure drop calculated with EGB GS 1999 the mass flow rate of the exhaust gases was not taken into account and was constant for all nine cases. GE2-Select took the mass flow rate into account and the results with it were more accurate and sensible.

The sales program that is used in Alfa Laval Aalborg Oy is used in dimensioning the waste heat recovery boilers and it is a part of the whole programs management system in Alfa

Laval Rauma office. In the sales tool the dual pressure solutions can be calculated as well as steam drums and WHR-boilers for various solutions.

Structure of the update block for the sales tool was presented and T-Q -diagrams generated with it were shown. Radiation from the exhaust gas to finned tubes was not necessary to be taken into account, because the impact of it is negligible compared to the total amount of heat transfer.

REFERENCES

Aalborg Industries. 1995. ABC-design dimensioning program. Property of Alfa Laval Aalborg Oy

Alfa Laval Aalborg Oy. 1998. Aalborg Industries Spiral Wound Fin Tubes Design Manual. Property of Alfa Laval Aalborg Oy

Alfa Laval Aalborg Oy. 1999. EGB GS 1999 dimensioning program. Property of Alfa Laval Aalborg Oy

Alfa Laval Aalborg Oy. 2000. WHR Boiler Select dimensioning program. Property of Alfa Laval Aalborg Oy

Alfa Laval Aalborg Oy. 2017. iPro mindmap. Property of Alfa Laval Aalborg Oy

Alfa Laval Aalborg Oy. 2018. iPro -dimensioning program. Property of Alfa Laval Aalborg Oy

Altosole Marco, Benvenuto Giovanni, Campora Ugo, Laviola Michele & Trucco Alessandro. 2017. Waste Heat Recovery from Marine Gas Turbines and Diesel Engines. Genova, Italy: University of Genoa & Fincantieri S.p.A. [referenced 2.11.2018]. Available ProQuest

Carcasci Carlo, Ferraro Riccardo, Miliotti Edoardo. 2014. Thermodynamic analysis of an organic Rankine cycle for waste heat recovery from gas turbines. Florence, Italy: University of Florence. [referenced 21.12.2018]. Available Elsevier

Incropera Franck P., Bergmann Theodore L., Lavine Adrienne S. & Dewitt David P. 2011. Fundamentals of Heat and Mass Transfer. Seventh edition. United States of America: John Wiley & Sons, Inc. ISBN 13 9778-0470-50197-9

Kehlhofer Ralf, Rukes Bert, Hannemann Frank & Stirnimann Franz. 2009. Combined-Cycle Gas & Steam Turbine Power Plants. 3rd Edition. Tulsa, United States of America: PennWell Corporation. 391 pages. ISBN 978-1-59370-168-0

Khan M.N., Tlili I. & Khan W.A. 2017. Thermodynamic Optimization of New Combined Gas/Steam Power Cycles with HRSG and Heat Exchanger. Majmaah, Kindom of Saudi Arabia: College of Engineering, Majmaah University. [referenced 5.2.2019]. Available SpringerLink

Li Yongui, Zhang Guoqiang, Bai Ziwei, Song Xiaowei, Wang Ligang & Yang Yongping, 2018. Backpressure adjustable gas turbine combined cycle: A method to improve part-load efficiency. Beijing, China: North China Electric Power University. Sion, Switzerland: Swiss Federal Institute of Technology of Lausanne. [referenced 5.2.2019]. Available Elsevier

Läiskä Pekka. 2001. GE2-Select dimensioning program. Property of Alfa Laval Aalborg Oy

Quoilin Sylvain, Ven Den Broek Martijn, Declaye Sébastien, Dewallef Pierre & Lemort Vincent. 2013. Techno-economic survey of Organic Rankine Cycle (ORC) systems. Liége, Belgium: University of Liége. Gent, Belgium: Ghent University-Ugent. [referenced 4.3.2019]. Available Elsevier

Raiko Risto, Saastamoinen Jaakko, Hupa Mikko & Kurki-Suonio Ilmari, 2002. Poltto ja palaminen. Helsinki, Finland: Teknillistieteelliset akatemiat – De tekniskvetenskapliga akademierna r.y. 750 s. ISBN 951-666-604-3

Roy J.P., Mishra M.K. & Misra Ashok. 2010. Parametric optimization and performance analysis of a waste heat recovery system using Organic Rankine Cycle. Bhagalpur and Mesra, India: NTPC Limited Kahalgaon and Birla Institute of Technology. [referenced 21.12.2018]. Available Elsevier

Saghafifar Mohammad, Gadalla Mohamed, 2015. Analysis of Maisotsenko open gas turbine bottoming cycle. Sharjah, United Arab Emirates: American University of Sharjah. [referenced 5.2.2019]. Available Elsevier

Sun Qingxuan, Wang Yaxiong, Cheng Ziyang, Wang Jiangfeng, Zhao Pan & Dai Yiping. 2018. Thermodynamic and economic optimization of a double-pressure organic Rankine cycle driven by low-temperature heat source. Xi'an, China: Xi'an Jiaotong University. [referenced 21.12.2018]. Available Elsevier

Usune Yoshie, Terazaki Masao, Tomita Yasuoki & Lee Jun-Hee, 2011. Higher Avaialbility of Gas Turbine Combined Cycle. Mitsubishi Power System Americas. [referenced 5.2.2019]. Available ProQuest

Youfu Ma, Lijuan Yang, Junfu Lu & Yufeng Pei, 2016. Techno-economic comparison of boiler cold end flue gas heat recovery processes for efficient hard-coal-fired power generation. Shanghai, China: University of Shanghai for Science and Technology, Tsinghua University & Northeast Electric Power Designing Institute, China Electric Power Engineering Consultancy Group. [referenced 4.11.2018]. Available ScienceDirect

Wang Chaojun, He Boshu, Sun Shaoyang, Wu Ying, Yan Na, Yan Lindo & Pei Xiaohui, 2012. Application of a low pressure economizer for waste heat recovery from the exhaust flue gas in a 600 MW power plant. Beijing, China: School of Mechanical, Electronical and Control Engineering, Beijing Jiaotong University, Beijing, China. [referenced 5.2.2019]. Available Elsevier

Weierman Chris. 1976. Correlations ease the selection of finned tubes. Okla, USA: Escoa Fintube Corporation. Property of Alfa Laval Aalborg Oy.

Zhang Hualing, Guan Xuan, Ding Yang & Liu Chao. 2018. Emergy analysis of Organic Rankine Cycle (ORC) for waste heat power generation. Chongqing, China: Chongqing University. [referenced 21.12.2018]. Available Elsevier